

Gas- and Solution-Phase Energetics of the Methyl  $\alpha$ - and  $\beta$ -D-Aldopentofuranosides

Justin B. Houseknecht, Todd L. Lowary,\* and Christopher M. Hadad\*

Department of Chemistry, The Ohio State University, Columbus, Ohio 43210

Received: December 13, 2002; In Final Form: March 31, 2003

The conformational preferences of the furanose rings in methyl  $\alpha$ -D-arabinofuranoside (**1**), methyl  $\beta$ -D-arabinofuranoside (**2**), methyl  $\alpha$ -D-lyxofuranoside (**3**), methyl  $\beta$ -D-lyxofuranoside (**4**), methyl  $\alpha$ -D-ribofuranoside (**5**), methyl  $\beta$ -D-ribofuranoside (**6**), methyl  $\alpha$ -D-xylofuranoside (**7**), and methyl  $\beta$ -D-xylofuranoside (**8**) have been studied in the gas (B3LYP/6-31+G\*\*//B3LYP/6-31G\*) and aqueous (B3LYP/6-31+G\*\*//SM5.42/BPW91/6-31G\*) phases. The results of these theoretical investigations are compared to previous theoretical and experimental results to determine the northern and southern minima in solution for each glycoside.

## Introduction

It has long been appreciated that the conformational preferences of biomolecules are important determinants of their biological activity. This realization has prompted an enormous amount of investigation in the areas of protein and DNA conformation, and more recently these studies have been extended to oligo- and polysaccharides.<sup>1</sup> Of particular importance to this paper is the increasing number of reports that have demonstrated the important role that substrate conformation plays in the regulation of the biological activity of nucleoside- and glycoside-processing enzymes. For example, Boons and co-workers recently demonstrated that large differences in the rate of sialylation of GlcNAc acceptors by rat liver  $\alpha$ -(2 $\rightarrow$ 6)-sialyltransferase can be substantially altered by varying the conformational preferences of the acceptor away from the unrestrained low-energy conformation.<sup>2</sup> Additionally, in a series of elegant papers, Marquez and co-workers have shown that biasing the conformation of the furanose ring in nucleosides can alter the ability of these molecules to act as substrates for various enzymes including adenosine deaminase, HIV-1 reverse transcriptase, and others.<sup>3</sup>

Several years ago we initiated a research program focused on obtaining a better understanding of the conformational preferences of the D-arabinofuranose ring system through experimental and theoretical methods.<sup>4</sup> The critical role that the arabinofuranose ring system plays in the cell wall structure of mycobacteria, including those species responsible for the diseases leprosy and tuberculosis, prompted our interest in this area.<sup>5</sup> Our investigations were undertaken with the hope that a detailed understanding of the conformational preferences of oligosaccharides containing arabinofuranose rings would facilitate the design and synthesis of potent inhibitors of the enzymes involved in mycobacterial cell wall biosynthesis.

The model we used to describe the conformational preferences of the furanose rings in these molecules was the one developed by Altona and Sundaralingam for ribonucleosides.<sup>6</sup> This model makes use of the pseudorotational wheel (Figure 1) to describe the possible ring conformers. Structurally similar conformers are located near one another on the wheel such that only small

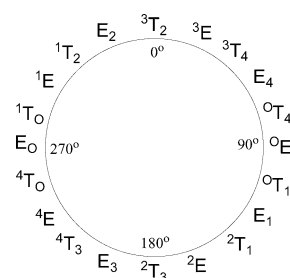


Figure 1. Pseudorotational itinerary for a D-aldofuranose ring.

conformational distortions between twist (T) and envelope (E) conformers are required for pseudorotation between adjacent conformers. Atoms that lie above the plane are denoted with a superscript and those that lie below the plane by a subscript. For a given furanose ring, the model assumes a dynamic equilibrium of two conformers, one in the northern hemisphere of the pseudorotational wheel and the other in the southern hemisphere, termed, respectively, the northern (N) and southern (S) conformers.

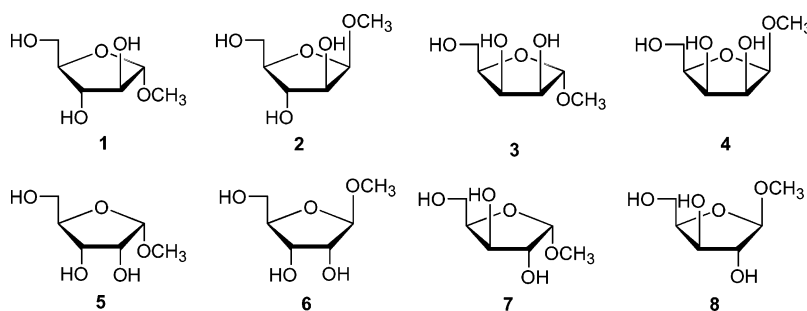
Recently, we became interested in extending our conformational studies to other aldopentofuranosides (**1–8**, Chart 1).<sup>4a,b</sup> Our investigations to date have enabled us to improve and clarify the results obtained by analysis of  $^3J_{\text{H,H}}$  data with the program PSEUROT,<sup>8</sup> not only for the arabinofuranose ring, but also for other aldopentofuranosides. These studies have also, however, underscored the complexity of understanding the conformational preferences of some of these ring systems from NMR data alone. Therefore, using computational methods, we have studied the conformational preferences of **1–8** both in the gas phase and in a model of aqueous solution. We report here the results of these computational investigations. In our studies we have employed the locked-envelope method, which has been used successfully by both us and others to study the conformation of furanose ring systems.<sup>4c–e,7</sup>

## Methods

Density functional theory (DFT) calculations were performed using Gaussian 98<sup>9</sup> and the MN-GSM solvation method.<sup>10</sup> For each methyl furanoside **1–8**, 30 idealized envelope conformers were generated in both the gas (B3LYP/6-31G\*)<sup>11</sup> and solution (SM5.42/BPW91/6-31G\*)<sup>12</sup> phases as previously reported.<sup>4a</sup> For

\* To whom correspondence should be addressed. E-mail: lowary.2@osu.edu, hadad.1@osu.edu.

## CHART 1



each ring system 1–8, three series of 10 idealized envelope geometries (a total of 30 structures) were constructed differing only in the orientation about the C<sub>4</sub>–C<sub>5</sub> bond. In one series, the orientation of this C<sub>4</sub>–C<sub>5</sub> bond was gg, another gt, and the third tg (Figure 2a). In all conformers, the aglycone was placed

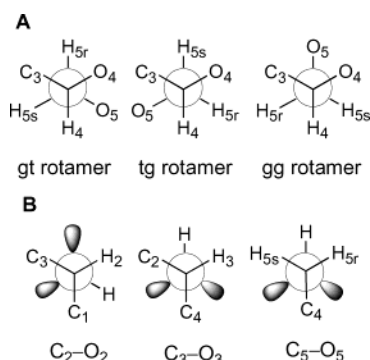


**Figure 2.** (a) Definition of gg, gt, and tg rotamers about the C<sub>4</sub>–C<sub>5</sub> bond. (b) Initial orientations about the C–O bonds.

in the position favored by the exo-anomeric effect, antiperiplanar to C<sub>2</sub>.<sup>13</sup> The orientations of the hydroxyl hydrogens were initially set as follows: OH<sub>2</sub> anti to C<sub>3</sub>, OH<sub>3</sub> anti to C<sub>4</sub>, and OH<sub>5</sub> anti to C<sub>4</sub> (Figure 2b). Each geometry was optimized first at the B3LYP/6-31G\* level in the gas phase and then at the SM5.42/BPW91/6-31G\* level for aqueous solvation with a single endocyclic dihedral angle fixed at 0° to maintain the envelope ring conformation. All of the other geometric parameters (bond distances, bond angles, and dihedral angles) were allowed to fully optimize. Upon gas-phase minimization, the orientation about the exocyclic C–O bonds for some conformers changed. These changes were generally to a position more favorable for the formation of intramolecular H-bonds. Where these changes occurred, they are noted below in the text. For the C<sub>1</sub>–O<sub>1</sub> or C<sub>4</sub>–C<sub>5</sub> bond, no substantial rotameric changes were observed; however, slight deviations away from ideally staggered orientations were sometimes found. Single-point energies were then determined for both the gas- and solution-phase geometries at the B3LYP/6-31+G\*\* level of theory using the appropriate geometries. We,<sup>4d–g</sup> and others,<sup>14</sup> have shown that the inclusion of such a single-point energy is critical for providing better relative energies for intramolecularly hydrogen-bonded systems. The solution-phase energy of each conformer was approximated using eqs 1 and 2. The geometrical data for these conformers were analyzed using the program ConforMole.<sup>15</sup>

$$\Delta G_{\text{solvation}} = E_{\text{SM5.42/BPW91/6-31G}^*} - E_{\text{BPW91/6-31G}^*(\text{gas})} \quad (1)$$

$$E_{\text{B3LYP/6-31+G}^{**}/\text{SM5.42/BPW91/6-31G}^*(\text{solution})} = E_{\text{B3LYP/6-31+G}^{**}/\text{SM5.42/BPW91/6-31G}^*(\text{gas})} + \Delta G_{\text{solvation}} \quad (2)$$

## Results

**A. Methyl  $\alpha$ -D-Arabinofuranoside (1).** *Geometrical Preferences.* Optimization of the 30 locked-envelope conformers of **1** was not without difficulty. In fact, it was not possible to obtain an optimized geometry for the <sup>4</sup>E-gg and E<sub>3</sub>-gg ring conformers by locking a single ring dihedral angle in either the gas or solution phase. At both the B3LYP/6-31G\* and SM5.42/BPW91/6-31G\* levels of theory, these conformers flipped from the <sup>4</sup>E or E<sub>3</sub> ring conformer to either the E<sub>4</sub> or <sup>3</sup>E ring form, respectively. The low barrier for ring interconversion through the planar form may be caused by the high energy of placing the C<sub>4</sub>-hydroxymethyl group in a pseudoaxial position, particularly for the gg C<sub>4</sub>–C<sub>5</sub> rotamer in which OH<sub>5</sub> is over the ring. The 28 gas-phase conformers of **1** were not substantially stabilized by H-bonds. The <sup>1</sup>E and <sup>3</sup>E ring conformers were stabilized by weak O<sub>2</sub>–H···O<sub>1</sub> and O<sub>3</sub>–H···O<sub>2</sub> H-bonds, respectively, in the gas phase. The E<sub>2</sub> ring conformer was stabilized by both these H-bonds. Optimization of these conformers with the SM5.42 solvation model resulted in both a lengthening of the H-bonds and a narrowing of the angle, suggesting an overall weakening of the geometrical importance of these interactions in solution. The puckering amplitudes ( $\Phi_m$ ) of all of the gas- and aqueous-phase geometries of **1** were within a range of 20–41° (Table 1). The average  $\Phi_m$  for the solution-

**TABLE 1: Range and Average Value of Puckering Amplitudes Present in 1–8 in the Gas and Aqueous Phases**

compd	gas $\Phi_m$	gas $\Phi_m$	soln $\Phi_m$	soln $\Phi_m$
	range		range	
	(deg)	av (deg)	(deg)	av (deg)
<b>1</b>	20–41	34.8	22–40	35.0
<b>2</b>	23–39	34.5	24–40	35.8
<b>3</b>	29–42	36.6	28–43	37.4
<b>4</b>	26–43	32.5	25–44	33.9
<b>5</b>	27–42	32.4	28–42	33.6
<b>6</b>	23–43	36.2	21–43	36.2
<b>7</b>	31–40	36.1	30–43	37.3
<b>8</b>	25–42	36.4	24–43	36.7

phase geometries (35.0°) was slightly greater than that of the gas-phase conformers of **1** (34.8°). Both the gas- and solution-phase conformers showed a marked dependence of  $\Phi_m$  upon the *P* value. The furanose rings in the southern <sup>2</sup>E, E<sub>3</sub>, <sup>4</sup>E, and E<sub>0</sub> ring conformers were uniformly flatter than all of the other ring forms by approximately 5°. This was likely due to steric interactions arising from the pseudoaxial placement of the secondary hydroxyl groups and the C<sub>4</sub>-hydroxymethyl group in these conformers, which can be alleviated by flattening of the furanose ring (see the Supporting Information, Figure S9).

*Energetic Profiles.* The gas- and solution-phase energy diagrams of **1** are shown in Figure 3. The gas-phase energy diagram (Figure 3a) at the B3LYP/6-31+G\*\*//B3LYP/6-31G\* level of theory has a predictable shape. The conformers in which the furanose ring was locked in the northeastern portion of the

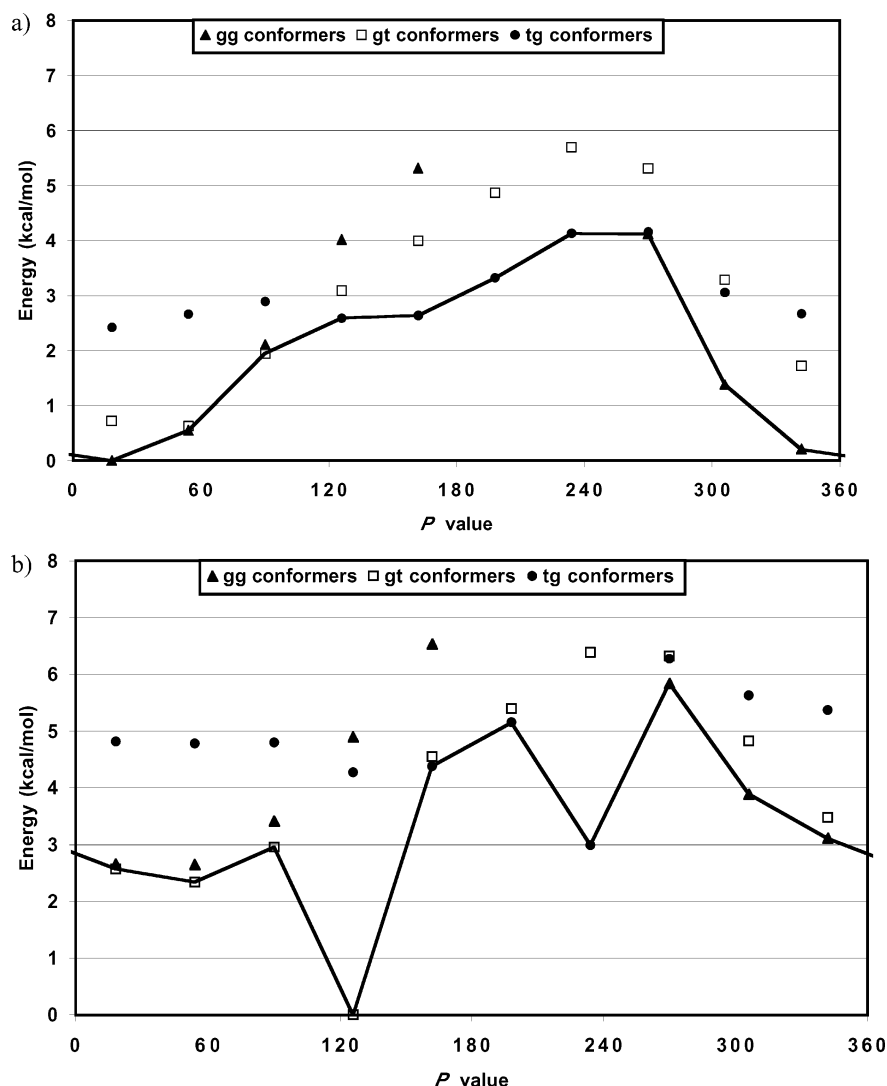


**Figure 3.** (a) Gas-phase relative energy profile of **1** at the B3LYP/6-31+G\*\*//B3LYP/6-31G\* level of theory. (b) Solution-phase relative energy profile of **1** at the B3LYP/6-31+G\*\*//SM5.42/BPW91/6-31G\* level of theory. See Figure 2 for the definitions of the gg, gt, and tg rotamers about the C<sub>4</sub>–C<sub>5</sub> bond. The line drawn connects the lowest energy rotamer for each ring form.

pseudorotational itinerary are the lowest energy structures. This was expected as the C<sub>4</sub>-hydroxymethyl group is in an equatorial position in the <sup>3</sup>E and E<sub>4</sub> ring conformers. In the gas phase, the lowest energy conformers, E<sub>2</sub>-gg and <sup>3</sup>E-gg, were stabilized by weak H-bonds and also benefit from a pseudoequatorial placement of the OH<sub>2</sub> and OH<sub>3</sub> (Figure 4a). The lowest energy geometries in the south were the E<sub>1</sub>-tg and <sup>2</sup>E-tg conformers (Figure 4a). Although 2.6 kcal/mol above the global minimum, they were stabilized by placement of the aglycone in a pseudoaxial orientation as preferred by the anomeric effect. The geometries in the western portion of the pseudorotational itinerary were, as expected, highest in energy. The pseudoaxial placement of the C<sub>4</sub>-hydroxymethyl group in these conformers was particularly disfavored for the gg C<sub>4</sub>–C<sub>5</sub> rotamer as demonstrated by the difficulty in isolating two of the three ring conformers (E<sub>3</sub> and <sup>4</sup>E) which place this group in this orientation (see above).

When the conformers of **1** were optimized using the SM5.42 solvation model, the primary result was a decrease in strength of intramolecular H-bonds, as discussed below. The global minimum at the B3LYP/6-31+G\*\*//SM5.42/BPW91/6-31G\* level of theory was the E<sub>1</sub>-gt conformer (Figures 3b and 4a). This S minimum-energy ring conformer was expected to be a low-energy structure as it places the aglycone in the position

favored by the anomeric effect. In solution, the E<sub>1</sub>-gt conformer was of substantially lower relative energy than in the gas phase, and we are unsure as to the origin of this decrease. The N minimum in solution, the E<sub>4</sub> ring conformer, was also expected to be a low-energy ring conformer as the C<sub>4</sub>-hydroxymethyl group is oriented equatorially (Figure 4a). The lowest energy C<sub>4</sub>–C<sub>5</sub> rotamer for all of the low-energy N ring conformers was gt. The gt conformers had a higher solution-phase dipole moment (average 3.4 D) than the gg and tg conformers (1.1 and 3.2 D, respectively), which may explain their increased stability in the SM5.42 model of aqueous solution. The western ring conformers are still higher energy structures than those in the east, although the E<sub>O</sub>-tg conformer was of significantly lower energy in solution (Figure 3b). Regardless, the western ring conformers are still disfavored and are unlikely to contribute to the Boltzmann distribution in aqueous solution.

**Comparison to Previous Studies.** The N and S solution minima found in this investigation agree well with previous studies (Table 2). The crystal structure reported for **1** has an E<sub>4</sub> ring structure, and the N minimum found at the B3LYP/6-31+G\*\*//SM5.42/BPW91/6-31G\* level of theory was E<sub>4</sub>-gt and had the same  $\Phi_m$  as the crystal structure.<sup>16</sup> The identities of the N and S minima are also the same as those previously predicted by analysis of <sup>1</sup>H NMR spectra<sup>4a</sup> (E<sub>4</sub> and E<sub>1</sub>) and similar to

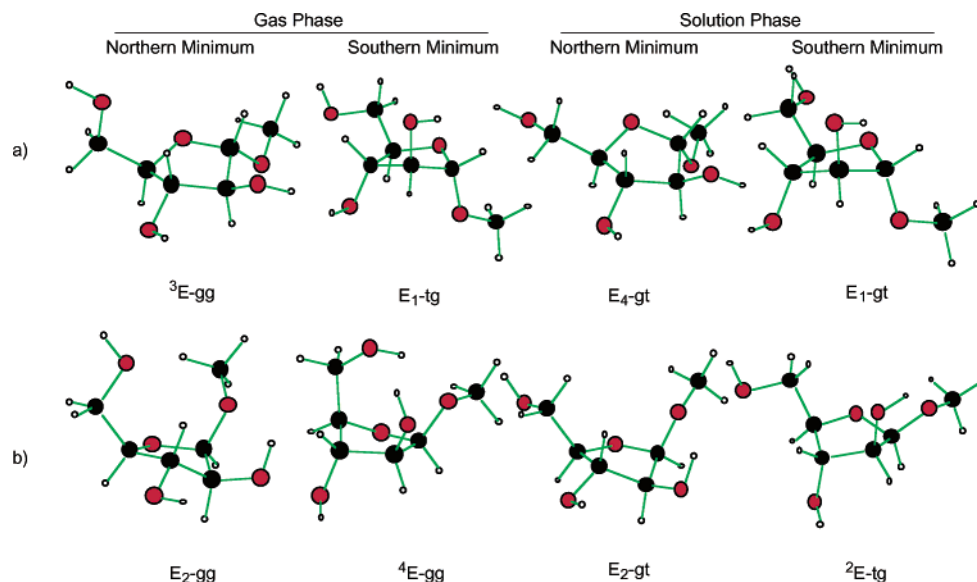


**Figure 4.** Northern and southern minima of (a) **1** and (b) **2** at the B3LYP/6-31+G\*\*//B3LYP/6-31G\* (gas) and B3LYP/6-31+G\*\*//SM5.42/BPW91/6-31G\* (solution) levels of theory.

**TABLE 2: Conformational Preferences of the Furanose Rings in 1–8 As Determined by This Study,  $^3J_{\text{H,H}}$  and  $^3J_{\text{C,O,C,H}}$  Data,<sup>4b</sup> and X-ray Crystallography<sup>16,18</sup>**

compd	gas-phase minima		solution-phase minima		NMR conformer distribution				crystal structure
	north	south	north	south	north family	%N	south family	%S	
<b>1</b>	$^3\text{E}$	$\text{E}_1$	$\text{E}_4$	$\text{E}_1$	$\text{E}_4$	39	$\text{E}_1$	61	$\text{E}_4$
<b>2</b>	$\text{E}_2$	$^4\text{E}$	$\text{E}_2$	$^4\text{E}$	$\text{E}_2$	87	$^2\text{E}$	13	$^1\text{T}_2$
<b>3</b>	$\text{E}_2$	$^2\text{E}$	$^0\text{E}$	$\text{E}_3$	$^3\text{E}$	65	$^4\text{T}_3$	35	$^3\text{E}$
<b>4</b>	$^1\text{E}$	$^4\text{E}$	$\text{E}_2$	$^4\text{E}$	$\text{E}_2$	77	$^1\text{E}$	23	
<b>5</b>	$\text{E}_4$	$^2\text{E}$	$\text{E}_4$	$^2\text{E}$			$\text{E}_1$	100	
<b>6</b>	$^3\text{E}$	$^4\text{E}$	$^1\text{E}$	$^4\text{E}$	$\text{E}_2$	86	$^0\text{E}$	14	$\text{E}_2$
<b>7</b>	$^0\text{E}$	$^2\text{E}$	$^3\text{E}$	$\text{E}_1$			$\text{E}_1$	100	$^2\text{E}$
<b>8</b>	$\text{E}_2$	$\text{E}_3$	$\text{E}_2$	$^4\text{E}$	$\text{E}_2$	78	$^4\text{T}_0$	22	

those from more extensive gas-phase computational methods ( $^3\text{T}_4$  and  $^2\text{T}_1$ ).<sup>4d,e</sup>

**B. Methyl  $\beta$ -D-Arabinofuranoside (**2**). Geometrical Preferences.** Optimization of the 30 ring conformers of **2** in both the gas and solution phases proceeded without difficulty. In almost all instances, however, the  $\text{OH}_2$  hydrogen rotated from its starting position (anti to the  $\text{C}_2\text{--C}_3$  bond) to H-bond to the aglycone oxygen. For three of the  $\text{C}_4\text{--C}_5$  gg rotamers ( $^2\text{E}$ ,  $^4\text{E}$ , and  $\text{E}_3$ ), a hydrogen-bonding network was formed in the gas-phase geometries among  $\text{OH}_2$ ,  $\text{OH}_5$ , and either the ring or aglycone oxygen ( $\text{O}_2\text{--H}\cdots\text{O}_5\text{--H}\cdots\text{O}_{4(1)}$ ). This hydrogen-bonding network was weakened for the  $^2\text{E}$  and  $\text{E}_3$  conformers upon optimization in aqueous solution as observed by a lengthening of the distance between  $\text{O}_5$  and the ring or aglycone oxygen, respectively, and a decrease in the corresponding  $\text{O--H}\cdots\text{O}$  angle. Interestingly, unlike what was observed with **1**, the average length and angle of the H-bonds present in the gas-phase geometries did not change significantly upon optimization in aqueous solvent. Ring puckering in the gas- and solution-phase conformers of **2** varied from  $23^\circ$  to  $40^\circ$  with average values of  $34.5^\circ$  and  $35.8^\circ$ , respectively (Table 1). The  $\text{E}_4\text{--tg}$  and  $\text{E}_0\text{--gg}$  conformers were significantly less puckered than the other 28 conformers with gas-phase  $\Phi_m$  values below  $27^\circ$ . Optimization at the SM5.42/BPW91/6-31G\* level of theory significantly increased the amount of pucker in the furanose ring of the  $\text{E}_4\text{--tg}$  conformer, but the  $\text{E}_0\text{--gg}$  conformer remained quite flat with a  $\Phi_m$  value of only  $24.5^\circ$ .

**Energetic Profiles.** The gas-phase energy distribution of **2** at the B3LYP/6-31+G\*\*//B3LYP/6-31G\* level of theory is quite different from that of **1** (compare Figures 3a and 5a). The global

minimum was the  $\text{E}_2\text{--gg}$  conformer (Figure 4b). This conformer was stabilized by a moderately strong H-bond between  $\text{OH}_2$  and  $\text{O}_1$ , pseudoequatorial orientation of the secondary hydroxyl groups, and pseudoaxial orientation of the aglycone. Another N conformer,  $^3\text{E}\text{--gg}$ , which was approximately 1 kcal/mol higher in energy, differed primarily in that it lacked the pseudoaxial orientation of the aglycone. The  $\text{E}_2\text{--gt}$  conformer was also of energy similar to that of the  $\text{E}_2\text{--gg}$  conformer, but the tg rotamer was significantly higher in energy, likely because it was the only conformer of **2** that was not stabilized by a H-bond of any type. H-bonding also played a major role in stabilization of the  $^2\text{E}\text{--gg}$ ,  $^4\text{E}\text{--gg}$ , and  $\text{E}_3\text{--gg}$  conformers. Figure 5a shows that these conformers formed a low-energy area in the southwestern portion of the pseudorotational itinerary, with the  $^4\text{E}$  ring conformer being the S minimum (Figure 4b). As discussed above, these conformers were stabilized by a strong H-bonding network in the gas phase. The relative energies of the gt and tg conformers suggest that the  $^2\text{E}$  ring conformers would likely be the S minima without the exaggerated stabilization of this H-bonding network. This was resolved when the effects of solvation on **2** were included.

The solution-phase energy diagram of **2** at the B3LYP/6-31+G\*\*//SM5.42/BPW91/6-31G\* level of theory is shown in Figure 5b. The global minimum was the same ring form seen in the gas phase,  $\text{E}_2$ , but the gt rotamer was lower in energy than the gg rotamer (Figure 4b). The  $\Phi_m$  of the  $\text{E}_2\text{--gt}$  conformer was  $37.8^\circ$ . The gt  $\text{C}_4\text{--C}_5$  rotamer was found to be either lower in energy or similar in energy to the gg rotamer for all of the ring conformers of **2** studied. This was in contrast to the gas-phase results, in which the gg rotamer was preferred, and

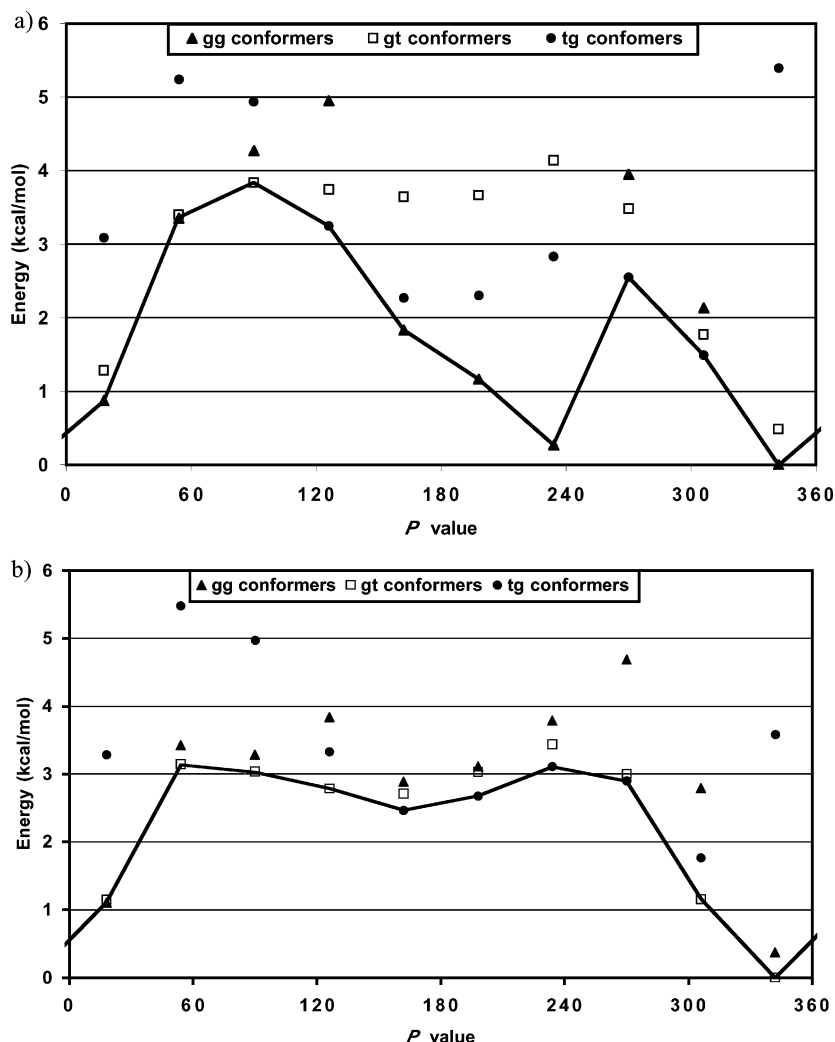


**Figure 5.** (a) Gas-phase relative energy profile of **2** at the B3LYP/6-31+G\*\*//B3LYP/6-31G\* level of theory. (b) Solution-phase relative energy profile of **2** at the B3LYP/6-31+G\*\*//SM5.42/BPW91/6-31G\* level of theory. See Figure 2 for the definitions of the gg, gt, and tg rotamers about the C<sub>4</sub>–C<sub>5</sub> bond. The line drawn connects the lowest energy rotamer for each ring form.

suggested that the gt rotamer is better able to interact with aqueous solvent than the gg C<sub>4</sub>–C<sub>5</sub> rotamer. The higher average dipole moment of the gt conformers (2.3 D) than the gg conformers (2.0 D) supports this argument. The southern portion of the pseudorotational itinerary was a largely flat, high-energy surface. For each C<sub>4</sub>–C<sub>5</sub> rotamer the lowest energy ring form was <sup>2</sup>E. The S minimum was the <sup>2</sup>E-tg conformer, which was stabilized by a moderate H-bond between OH<sub>2</sub> and the O<sub>1</sub> (Figure 4b). The gt and gg rotamers were 0.2 and 0.4 kcal/mol higher in energy, respectively. It should be noted that the three C<sub>4</sub>–C<sub>5</sub> rotamers (<sup>2</sup>E, <sup>4</sup>E, and E<sub>3</sub>) that were stabilized by a strong H-bonding network increased dramatically in energy in comparison to other conformers in the pseudorotational itinerary upon consideration of solvation effects and the conformer (E<sub>2</sub>-tg) which was not stabilized by any H-bonds decreased in energy. This was in agreement with intuition, which suggests that H-bonds should be less important in aqueous solvent than in the gas phase.

**Comparison to Previous Studies.** The results of this study are in agreement with other experimental and theoretical studies that have demonstrated that the lowest energy structure of **2** is between  $P = 325^\circ$  and  $P = 351^\circ$  (Table 2). The ring forms found by X-ray crystallography<sup>16</sup> and <sup>1</sup>H NMR studies,<sup>4a</sup> <sup>1</sup>T<sub>2</sub> and <sup>3</sup>T<sub>2</sub>, are on either side of the E<sub>2</sub> ring conformer found in this study. More extensive theoretical studies have also found

the major ring conformer to be in this region.<sup>4c</sup> The crystal structure of **2** had a  $\Phi_m$  of 0.39 Å (~0.39°), only 0.01 Å more than the solution-phase global minimum in the current study. All computational investigations of **2** have found the S conformer to be only a minor contributor to the Boltzmann distribution. No crystal structure of a southern ring form of **2** has been published, but <sup>1</sup>H NMR studies suggest that either the E<sub>3</sub> or <sup>2</sup>E ring form is present as approximately 10% of the aqueous distribution. However, this study, and previous theoretical approaches,<sup>4d,17</sup> have found the <sup>2</sup>E ring conformer to be slightly lower in energy than the E<sub>3</sub> ring conformer.

**C. Methyl α-D-Lyxofuranoside (3).** *Geometrical Preferences.* Optimization of the 30 conformers of **3** at the B3LYP/6-31G\* level of theory produced a family of conformers with substantial H-bonding. This was anticipated as all three hydroxyl groups are oriented cis and are therefore well situated for the formation of intramolecular H-bonds. The strongest and most prevalent H-bonding interactions were O<sub>3</sub>–H...O<sub>2</sub> and O<sub>5</sub>–H...O<sub>3</sub>. Several conformers did, however, also have O<sub>5</sub>–H...O<sub>2</sub> or O<sub>3</sub>–H...O<sub>5</sub> H-bonding, and the <sup>1</sup>E, E<sub>2</sub>, and <sup>3</sup>E ring conformers were further stabilized by a weak H-bond from OH<sub>2</sub> to O<sub>1</sub>. The latter interaction was only possible in ring conformers that situated OH<sub>2</sub> pseudoequatorial and therefore closer to O<sub>1</sub>. Optimization of the gas-phase conformers of **3** at the SM5.42/BPW91/6-31G\* level of theory did not significantly alter the



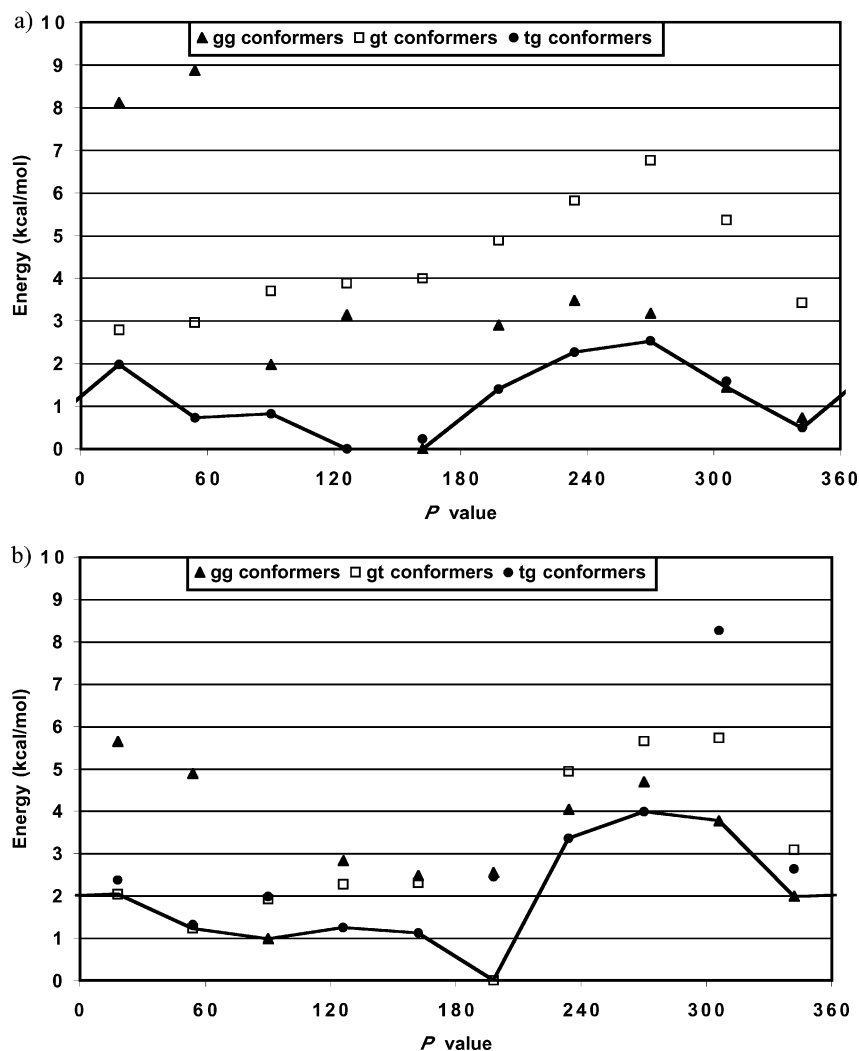


**Figure 6.** (a) Gas-phase relative energy profile of **3** at the B3LYP/6-31+G\*\*//B3LYP/6-31G\* level of theory. (b) Solution-phase relative energy profile of **3** at the B3LYP/6-31+G\*\*//SM5.42/BPW91/6-31G\* level of theory. See Figure 2 for the definitions of the gg, gt, and tg rotamers about the C<sub>4</sub>–C<sub>5</sub> bond. The line drawn connects the lowest energy rotamer for each ring form.

geometries. The length and angle of the H-bonds remained virtually unchanged, although most H-bonds grew slightly stronger (shorter OH...O distance, more linear OH...O angle) upon optimization in aqueous solvent. Puckering of the furanose rings of **3** did not differ significantly between the gas and aqueous phases. The only conformer with a  $\Phi_m$  less than 32° was the E<sub>3</sub>-tg conformer, which had a  $\Phi_m$  of approximately 29°. The maximum  $\Phi_m$  was 42.7° in the solution-phase geometry of the E<sub>4</sub>-gg conformer. Optimization at the SM5.42/BPW91/6-31G\* level of theory caused the average ring puckering to increase slightly from 36.6° in the gas phase to 37.4° in solution (Table 1).

**Energetic Profiles.** The gas-phase energy distribution of **3** is shown in Figure 6a. The most general and striking feature of this energy profile was that for almost every envelope conformer the lowest energy C<sub>4</sub>–C<sub>5</sub> rotamer was tg and the highest energy C<sub>4</sub>–C<sub>5</sub> rotamer was gt. This was entirely due to the increased ability of the tg rotamers to form a H-bond from OH<sub>5</sub> to O<sub>3</sub> and the inability of the gt rotamer to form a H-bond between OH<sub>5</sub> and either O<sub>2</sub> or O<sub>3</sub>. Although in the gt conformers OH<sub>5</sub> could have formed a H-bond to O<sub>4</sub>, this was not observed. The remarkably high energy of the <sup>3</sup>E-gg and E<sub>4</sub>-gg conformers was similarly a result of decreased H-bonding stabilization relative to that of the other 28 conformers. The lowest energy structures at the B3LYP/6-31+G\*\*//B3LYP/6-31G\* level of theory were

the E<sub>1</sub>-tg, <sup>2</sup>E-gg, and <sup>2</sup>E-tg conformers (Figure 7a). These three conformers were stabilized by a moderately strong H-bonding network from OH<sub>5</sub> to O<sub>3</sub> and from OH<sub>3</sub> to O<sub>2</sub>. These ring forms were further stabilized by placement of the aglycone and OH<sub>2</sub> in stereoelectronically favored axial or pseudoaxial positions, respectively. The gas-phase N minimum-energy structures were the gg and tg conformers of the E<sub>2</sub> ring conformer (Figure 7a), although the tg conformers of the <sup>0</sup>E and E<sub>4</sub> ring forms were only slightly higher in energy.

The solution-phase energy distribution of **3** was likely more realistic as the B3LYP/6-31+G\*\*//SM5.42/BPW91/6-31G\* level of theory dealt better with the effect of H-bonds than the gas-phase calculations, which exaggerated the amount of stabilization derived from H-bonds. The solution energy distribution of **3** (Figure 6b) did not favor or disfavor a particular C<sub>4</sub>–C<sub>5</sub> rotamer as seen in the gas phase. The global minimum E<sub>3</sub>-gt conformer was stabilized by a single H-bond from OH<sub>3</sub> to O<sub>2</sub> (Figure 7a). This conformer may also receive stabilization from the gauche effect with the ring oxygen as OH<sub>2</sub> is oriented pseudoaxially. The precise identity of the N minimum could not be determined from this study as several low-energy conformers exist in the eastern portion of the pseudorotational itinerary. The <sup>0</sup>E-gg conformer is the N minimum 1.0 kcal/mol above the global minimum (Figure 7a), but the gt and tg conformers of the E<sub>4</sub> ring form are just 0.2 and 0.3 kcal/mol

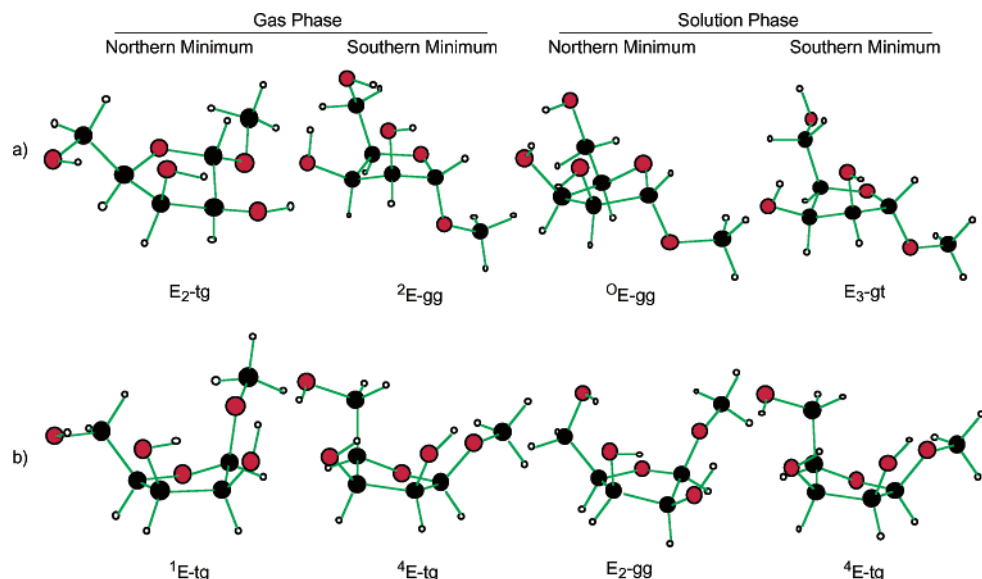


**Figure 7.** Northern and southern minima of (a) **3** and (b) **4** at the B3LYP/6-31+G\*\*//B3LYP/6-31G\* (gas) and B3LYP/6-31+G\*\*//SM5.42/BPW91/6-31G\* (solution) levels of theory.

higher in energy, respectively. Such small energetic differences are not particularly meaningful, especially in structures that were optimized with a geometrical constraint. Regardless, these conformers were significantly lower in energy than the other northern and western ring forms and should constitute the northern minimum in experimental studies. These conformers are stabilized by pseudoequatorial placement of the  $C_4$ -hydroxymethyl group and pseudoaxial placement of the aglycone.

**Comparison to Previous Studies.** The conformational preferences of **3** have not been studied as extensively as the arabinofuranose and ribofuranose ring systems, but this is not the first study of lyxofuranose conformational preferences. The crystal structure<sup>16</sup> of **3** is a  $^3E$  ring conformer, as is the N, and global, minimum from analysis of  $^3J_{H,H}$  data<sup>4a</sup> (Table 2). Although the current study found the two adjacent envelope conformers,  $E_4$  and  $E_2$ , to be low-energy structures, the  $^3E$  ring conformer was not predicted to be a significant contributor to the solution distribution. This may be the result of insufficient sampling of the conformational space in the current study. The crystal structure of **3** had a  $\Phi_m$  of  $0.43^\circ$  ( $\sim 43^\circ$ ), which is substantially greater than that of the other crystalline methyl aldopentofuranosides. Similarly, the current study also found the furanose ring of **3** to be more highly puckered than the other seven furanose ring systems examined (Table 1). Analysis of  $^3J_{H,H}$  data alone could not determine the identity of the S minimum, but recently we used  $^3J_{Cl,H4}$  to clarify that the  $^4T_3$  ring conformer was more likely than the  $^2T_1$  conformer.<sup>4b</sup> This proposal is validated by the current study, which found the global minimum to be the  $E_3$  ring conformer, the one adjacent to the conformer found by analysis of the  $^3J_{H,H}$  and  $^3J_{C,H}$  data (Table 2). The only previous theoretical study of the conformational preferences of **3** used fewer starting geometries, but did allow complete geometry optimization, and is therefore an interesting complement to this study.<sup>18</sup> In that investigation Evdokimov and co-workers found a  $^2E$  southern and global minimum and an  $E_4$  northern minimum. These results are in qualitative agreement with the current study, although it should be noted that, without more extensive geometric sampling, comparisons of this nature are of limited value.

**D. Methyl  $\beta$ -D-Lyxofuranoside (4).** *Geometrical Preferences.* The 30 optimized gas-phase conformers of **4** were the most strongly H-bonded of the eight compounds investigated.

Almost every gg and tg conformer was stabilized by an  $O_5-H\cdots O_3-H\cdots O_2-H\cdots O_1$  H-bonding network. The exceptions to this trend were the gg rotamers of the  $E_1$ ,  $^2E$ ,  $E_3$ , and  $^4E$  ring conformations in which  $OH_2$  was H-bonded to  $O_5$  instead of  $O_1$ . The  $E_3$ -gg and  $^4E$ -gg conformers further differed from the other 28 conformers of **4** in that  $OH_5$  was H-bonded to  $O_1$  instead of  $O_3$ . It should also be noted that for each ring conformer the gt rotamers were stabilized by only two H-bonds ( $O_2-H\cdots O_1$  and  $O_3-H\cdots O_2$ ). Optimization of the gas-phase conformers of **3** at the SM5.42/BPW91/6-31G\* level of theory did not dramatically change most of the geometries. For example, the length and angle of most of the H-bonds became stronger (e.g., shorter and wider) upon optimization in aqueous solvent. However, several of the H-bonds that were relatively weak in the gas phase relaxed significantly upon optimization in aqueous solution. The H-bond between  $OH_5$  and  $O_3$  in the  $^2E$ -gg,  $^3E$ -tg, and  $E_4$ -tg conformers increased in length by more than  $0.5 \text{ \AA}$ , and the H-bond between the  $OH_5$  and  $O_1$  increased in length by  $0.34 \text{ \AA}$ . These rearrangements were also accompanied by decreases in the  $O-H\cdots O$  angle. The furanose rings of **4** were less highly puckered than those of its anomer **3**. The average gas-phase  $\Phi_m$  in **4** was  $32.5^\circ$ , and the puckering only increased to  $33.9^\circ$  upon optimization at the SM5.42/BPW91/6-31G\* level of theory. The range of  $\Phi_m$  values was  $25$ – $44^\circ$  (Table 1).

**Energetic Profiles.** The gas-phase energetic distribution of conformers (Figure 8a) was dissimilar from those discussed previously. This is most evident in the low energy of the western ring conformers relative to the energy of the eastern conformers. The net effect is an overall flattening of the potential energy surface. This can be explained, at least in part, by the preferred pseudoaxial placement of the aglycone, which is possible only in the northwestern portion of the pseudorotational itinerary. As seen in the gas-phase distribution of **3**, the gt rotamer was highly disfavored, likely as a result of its decreased H-bonding ability. The global minimum of **4** at the B3LYP/6-31+G\*\*//B3LYP/6-31G\* level of theory was the  $^1E$ -tg conformer (Figure 7b). This conformer was stabilized by three H-bonds, as discussed above, and an axial orientation of the aglycone. The  $E_0$  and  $E_2$  ring conformers were also low-energy structures, but the southern minimum was the  $^4E$ -tg conformer (Figure 7b). However, the  $^4E$ -gg conformer was only  $0.1 \text{ kcal/mol}$  higher in

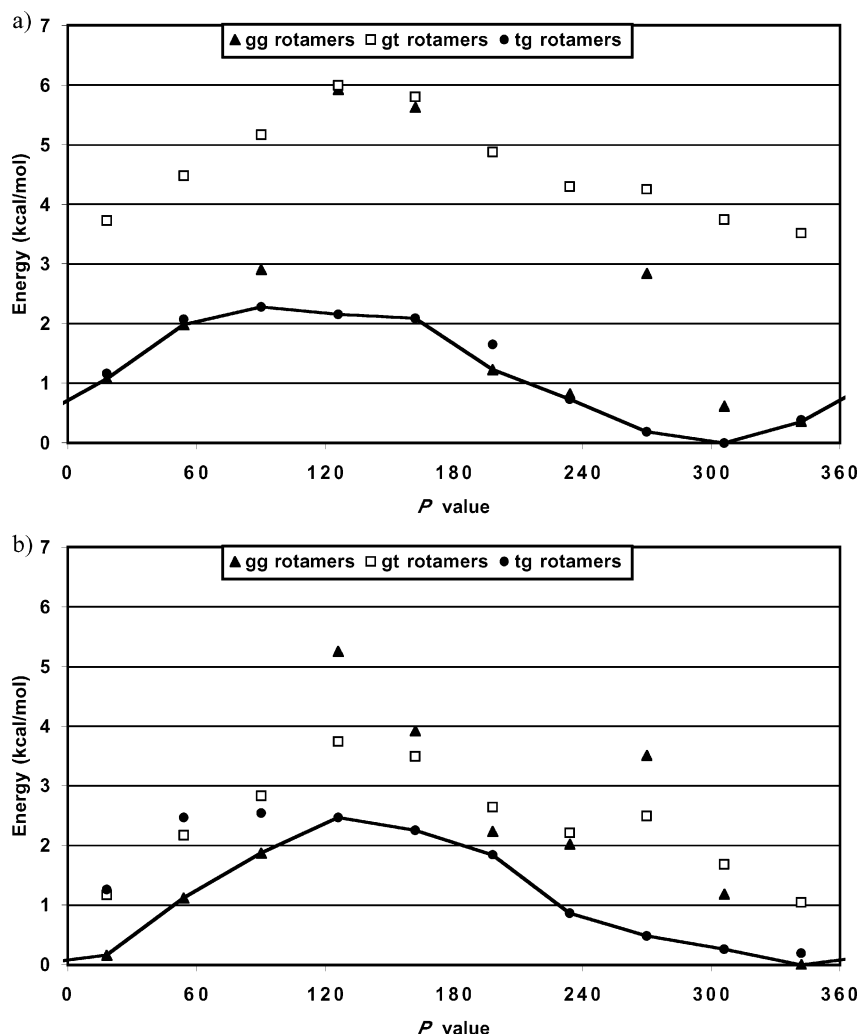


**Figure 8.** (a) Gas-phase relative energy profile of **4** at the B3LYP/6-31+G\*\*//B3LYP/6-31G\* level of theory. (b) Solution-phase relative energy profile of **4** at the B3LYP/6-31+G\*\*//SM5.42/BPW91/6-31G\* level of theory. See Figure 2 for the definitions of the gg, gt, and tg rotamers about the C<sub>4</sub>–C<sub>5</sub> bond. The line drawn connects the lowest energy rotamer for each ring form.

energy. The low energy of this ring conformer was unexpected as it placed the C<sub>4</sub>-hydroxymethyl group axial, but can best be understood in terms of the gg and tg rotamers' increased ability to form a strong network of H-bonds with minimal distortion of covalent bonds.

The general features of the energetic distribution of **4** at the B3LYP/6-31+G\*\*//SM5.42/BPW91/6-31G\* level of theory were similar to those in the gas phase (Figure 8b). The lowest energy conformers were in the northwestern portion of the pseudorotational itinerary, and the highest energy conformers were in the southeastern portion. The N minimum, however, was shifted slightly to the E<sub>2</sub>-gg conformer, which still placed the aglycone in a pseudoaxial orientation, but allowed the C<sub>4</sub>-hydroxymethyl group a less axial orientation (Figure 7b). The E<sub>2</sub>-gg conformer was stabilized by the same H-bonding network as most of the other conformers of **4** with no significant deviations in the distance or angle of H-bonding. The same could be said of the H-bond stabilization of the lowest energy conformer in the southern hemisphere, <sup>4</sup>E-tg (Figure 7b). The <sup>4</sup>E ring conformer was also the S minimum within each family of C<sub>4</sub>–C<sub>5</sub> rotamers (despite the unusual O<sub>2</sub>–H···O<sub>5</sub>–H···O<sub>3</sub>–H···O<sub>2</sub> H-bonding pattern present in the <sup>4</sup>E-gg conformer). The increased stability of this ring conformer was likely a result of its increased ability to form highly cooperative H-bonding networks.

**Comparison to Previous Studies.** To date, there has been little investigation of the conformational preferences of **4**. No X-ray crystal structure is available, and the analysis of <sup>3</sup>J<sub>H,H</sub> data by PSEUROT has been frustrated by multiple possible mathematical solutions. Recently, using <sup>3</sup>J<sub>Cl,H4</sub> data, we were able to eliminate several of the solutions found by analysis of only <sup>3</sup>J<sub>H,H</sub> data, but it remained unclear whether the solution distribution was a 3:1 mixture of the E<sub>2</sub> and <sup>1</sup>E ring conformers or a 3:2 mixture of the E<sub>4</sub> and E<sub>3</sub> ring conformers.<sup>4b</sup> The theoretical approach reported here agrees well with analysis of <sup>3</sup>J<sub>H,H</sub> and <sup>3</sup>J<sub>C,H</sub> data such that in solution, **4** exists as a 3:1 mixture of the E<sub>2</sub> and <sup>1</sup>E ring conformers (Table 2). The results of this approach also eliminate the E<sub>4</sub> and E<sub>3</sub> ring conformer solution on the basis of the relatively high energy of these ring forms as shown in Figure 8.

**E. Methyl α-D-Ribofuranoside (5). Geometrical Preferences.** Optimization of the 30 starting geometries of **5** at the B3LYP/6-31G\* level of theory proceeded without complication. In every instance, the hydrogens of OH<sub>2</sub> and OH<sub>3</sub> rotated to form a O<sub>3</sub>–H···O<sub>2</sub>–H···O<sub>1</sub> H-bonding network. This was expected and unavoidable due to the cis relationship of the secondary hydroxyl groups and the aglycone. Surprisingly, OH<sub>3</sub> did not H-bond to either O<sub>1</sub> or O<sub>4</sub> in any of the 30 conformers studied. The average length and angle of the O<sub>2</sub>–H···O<sub>1</sub> H-bond (1.92 Å, 121.4°) indicated that it was slightly stronger than the O<sub>3</sub>–H···O<sub>2</sub>



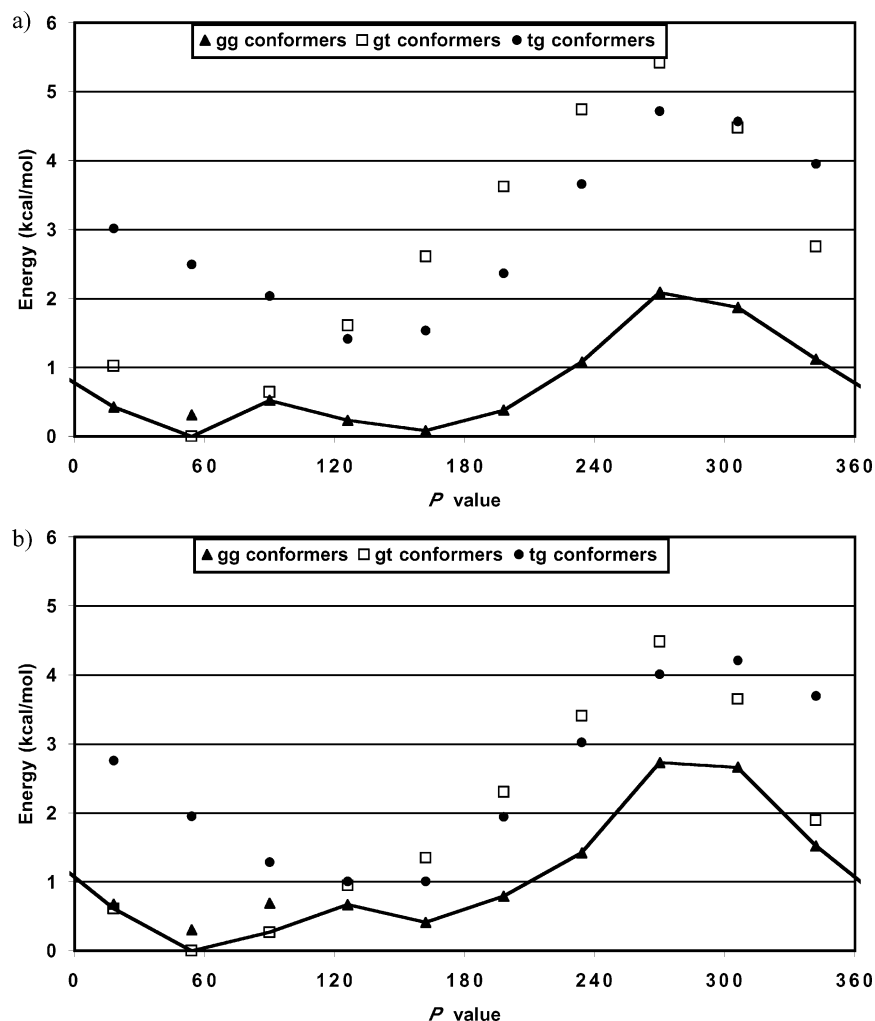


**Figure 9.** (a) Gas-phase relative energy profile of **5** at the B3LYP/6-31+G\*\*//B3LYP/6-31G\* level of theory. (b) Solution-phase relative energy profile of **5** at the B3LYP/6-31+G\*\*//SM5.42/BPW91/6-31G\* level of theory. See Figure 2 for the definitions of the gg, gt, and tg rotamers about the C<sub>4</sub>–C<sub>5</sub> bond. The line drawn connects the lowest energy rotamer for each ring form.

H-bond (2.00 Å, 120.2°). Optimization at the SM5.42/BPW91/6-31G\* level of theory caused only minor geometrical rearrangements, particularly as measured by H-bond arrangements. The average length of the O<sub>2</sub>–H···O<sub>1</sub> H-bond remained the same in aqueous solvent, but the bond angle widened slightly (to 122.6°), indicating a slight increase in H-bond strength. The average strength of the O<sub>3</sub>–H···O<sub>2</sub> H-bond also increased slightly (to 1.96 Å and 123.5°). This apparent strengthening of H-bonds at the SM5.42/BPW91/6-31G\* level of theory mirrors that seen in the other furanosides studied. The α-D-ribofuranosyl rings had  $\Phi_m$  values from 27° to 42° in the gas and solution phases (Table 1), and the average  $\Phi_m$  increased slightly from 32.4° to 33.6° upon optimization at the SM5.42/BPW91/6-31G\* level of theory. At both levels of theory, the ring conformers in the northeastern portion of the pseudorotational itinerary ( $P = 18$ –90°) were more highly puckered (average  $\Phi_m = 37.8^\circ$ ) than the other ring conformers (average  $\Phi_m = 31.0^\circ$ ; see the Supporting Information).

**Energetic Profiles.** Figure 9a illustrates the gas-phase energy distribution of **5**. The N (E<sub>4</sub>-gt) and S (E<sub>2</sub>-gg) minima were similar in energy, with the E<sub>2</sub>-gg conformer being only 0.1 kcal/mol higher in energy than the E<sub>4</sub>-gt conformer (Figures 9a and 10a). The E<sub>4</sub> ring conformer is stabilized by an equatorial orientation of the C<sub>4</sub>-hydroxymethyl group and the E ring conformer by a pseudoaxial orientation of the aglycone. The western portion of the pseudorotational itinerary was higher in

energy than the eastern region in large measure because of the undesirable orientation of the C<sub>4</sub>-hydroxymethyl group and the aglycone. The energy of the α-D-ribofuranosyl rings did not vary consistently as a function of  $\Phi_m$ , as detailed in the Supporting Information.

Optimization of the gas-phase geometries at the SM5.42/BPW91/6-31G\* level of theory led to no significant changes in the geometries. Due to the identical H-bonding pattern in all 30 conformers, the energetic distribution of **5** was not altered significantly either (Figure 9). The global and N minimum remained the E<sub>4</sub>-gt conformer (Figure 10a). The identity of the S minimum also remained the same, E<sub>2</sub>-gg, but it increased in energy relative to the N minimum. At the B3LYP/6-31+G\*\*//SM5.42/BPW91/6-31G\* level of theory, the S minimum was 0.4 kcal/mol higher in energy than the global minimum. The conformers in the western portion of the pseudorotational itinerary were still significantly higher in energy than the eastern conformers, suggesting that they would not contribute to the solution distribution of ring conformers.

**Comparison to Previous Studies.** The conformational preferences of the furanose ring in **5** have not been studied nearly as extensively as its β-anomer, **6**. No crystal structure is available for purposes of comparison, but analysis of  $^3J_{H,H}$  and  $^3J_{C,H}$  data suggests that **5** exists solely as the E<sub>1</sub> ring conformer in solution (Table 2).<sup>4b</sup> The present study did find the E<sub>1</sub> ring conformer to be the S minimum, but the global minimum, which is in the

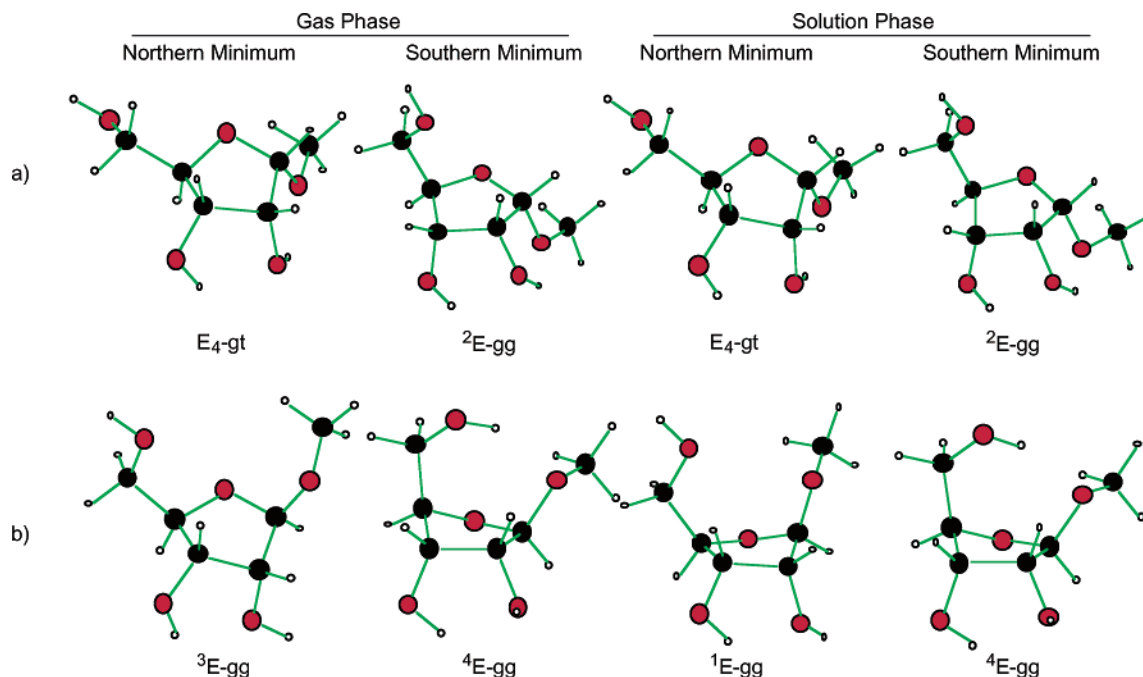


**Figure 10.** Northern and southern minima of (a) **5** and (b) **6** at the B3LYP/6-31+G\*\*//B3LYP/6-31G\* (gas) and B3LYP/6-31+G\*\*//SM5.42/BPW91/6-31G\* (solution) levels of theory.

northern hemisphere, was 0.5 kcal/mol lower in energy. This small energy difference could be attributed to insufficient sampling of the conformational space of **5**.

**F. Methyl  $\beta$ -D-Ribofuranoside (**6**). Geometrical Preferences.** Geometry optimization of the 30 conformers of **6** at the B3LYP/6-31G\* level of theory created a diversity of H-bonding patterns. The majority of conformers were stabilized by an O<sub>3</sub>–H $\cdots$ O<sub>2</sub> H-bond. E<sub>0</sub>-gt, E<sub>0</sub>-tg, and <sup>1</sup>E-tg, however, were stabilized by an O<sub>2</sub>–H $\cdots$ O<sub>3</sub> H-bond. Several gg rotamers were stabilized by a second H-bond from OH<sub>5</sub> to O<sub>1</sub> (<sup>4</sup>E and E<sub>3</sub>) or to O<sub>4</sub> (<sup>2</sup>E). All three C<sub>4</sub>–C<sub>5</sub> rotamers of the <sup>2</sup>E and E<sub>1</sub> conformers were stabilized by a weak H-bond from the OH<sub>2</sub> to the aglycone oxygen. The only conformer that was not stabilized by any H-bonds was the E<sub>2</sub>-gg conformer. Optimization of these gas-phase conformers at the SM5.42/BPW91/6-31G\* level of theory led to more reorganization than was observed in the other ring systems. The orientation of the <sup>1</sup>E-tg H-bond actually changed from O<sub>2</sub>–H $\cdots$ O<sub>3</sub> in the gas phase to O<sub>3</sub>–H $\cdots$ O<sub>2</sub> in solution. The orientation of the exocyclic bonds in other conformers remained the same, however, with the only significant change being a general shortening of all but two of the H-bonds. The H-bond involving OH<sub>5</sub> in the E<sub>3</sub>-gg and <sup>2</sup>E-gg conformers weakened as measured from 0.1 and 0.2 Å increases in length, respectively. The  $\Phi_m$  of the furanose ring in **6** varied from 21° to 43° with an average value of 36.2° (Table 1). The eastern <sup>0</sup>E and E<sub>1</sub> ring forms, however, were more puckered (average  $\Phi_m$  = 41.6°). The average  $\Phi_m$  of the  $\beta$ -D-ribofuranosyl ring did not change upon optimization at the SM5.42/BPW91/6-31G\* level of theory.

**Energetic Profiles.** The low-energy regions of the energetic distribution of **6** at the B3LYP/6-31+G\*\*//B3LYP/6-31G\* level of theory are dominated by strongly H-bonded conformers (Figure 11a). The S and global minimum-energy conformer, <sup>4</sup>E-gg, was one of three gg conformers stabilized by a moderately strong H-bond involving OH<sub>5</sub> (Figure 10b). The other two conformers, E<sub>3</sub>-gg and <sup>2</sup>E-gg, were also low-energy structures at this level of theory. The amount of stabilization received from the weak H-bond between OH<sub>2</sub> and O<sub>1</sub> appeared to be minimal as the <sup>2</sup>E and E<sub>1</sub> ring conformers were not

particularly low energy structures. The E<sub>2</sub>-gt and <sup>3</sup>E-gg ring conformers were both 3.1 kcal/mol above the global minimum and were the lowest energy northern ring conformers. Both were stabilized by a gauche interaction between the ring oxygen and one of the secondary hydroxyl groups. The E<sub>2</sub> ring conformer was further stabilized by the pseudoaxial orientation of the aglycone.

The energetic importance of H-bonds seemed to decrease in the solution-phase energy distribution of **6** (Figure 11b). The conformers, particularly <sup>4</sup>E-gg, with a strong H-bonding network remained low-energy structures, but the global minimum <sup>1</sup>E-gg conformer was stabilized by a single O<sub>3</sub>–H $\cdots$ O<sub>2</sub> H-bond (Figure 10b). The primary stabilization of the <sup>1</sup>E-gg conformer was from the axial orientation of the aglycone and a gauche interaction between the ring oxygen and the pseudoaxially located OH<sub>2</sub>. The E<sub>2</sub> and <sup>3</sup>E ring conformers were also low-energy N ring forms. As already mentioned, the <sup>4</sup>E-gg conformer was the S minimum-energy structure, largely due to stabilization from two moderate H-bonds (Figure 10b). The  $\Phi_m$  of this conformer increased to 35.0° in the solution phase.

**Comparison to Previous Studies.** The conformational preferences of **6** have been studied more extensively than those of the other methyl aldopentofuranosides due to the biological importance of nucleosides containing the  $\beta$ -D-ribofuranosyl ring. The crystal structure<sup>16</sup> and analysis of <sup>3</sup>J<sub>H,H</sub> data<sup>4b</sup> have found the E<sub>2</sub> ring conformer to be the dominant ring form in solution (Table 2). The present study found the E<sub>2</sub> ring form to be a low-energy structure, but the global minimum in solution was the adjacent <sup>1</sup>E ring form. The 0.4 kcal/mol difference between the two ring forms could easily be an artifact of the planar constraint used to lock each ring in an envelope geometry. Analysis of the <sup>3</sup>J<sub>H,H</sub> data also suggests that the S minimum is the <sup>0</sup>E ring form. However, it appears from the current study that the minor contributor to the Boltzmann distribution is more likely the <sup>4</sup>E ring conformer, but as it is such a minor contributor (<10%), it would be difficult to determine this experimentally. Ab initio studies of the conformational preferences of the reducing sugar  $\beta$ -D-ribofuranose produced results in qualitative agreement with the current study.<sup>7b</sup> In particular, both studies

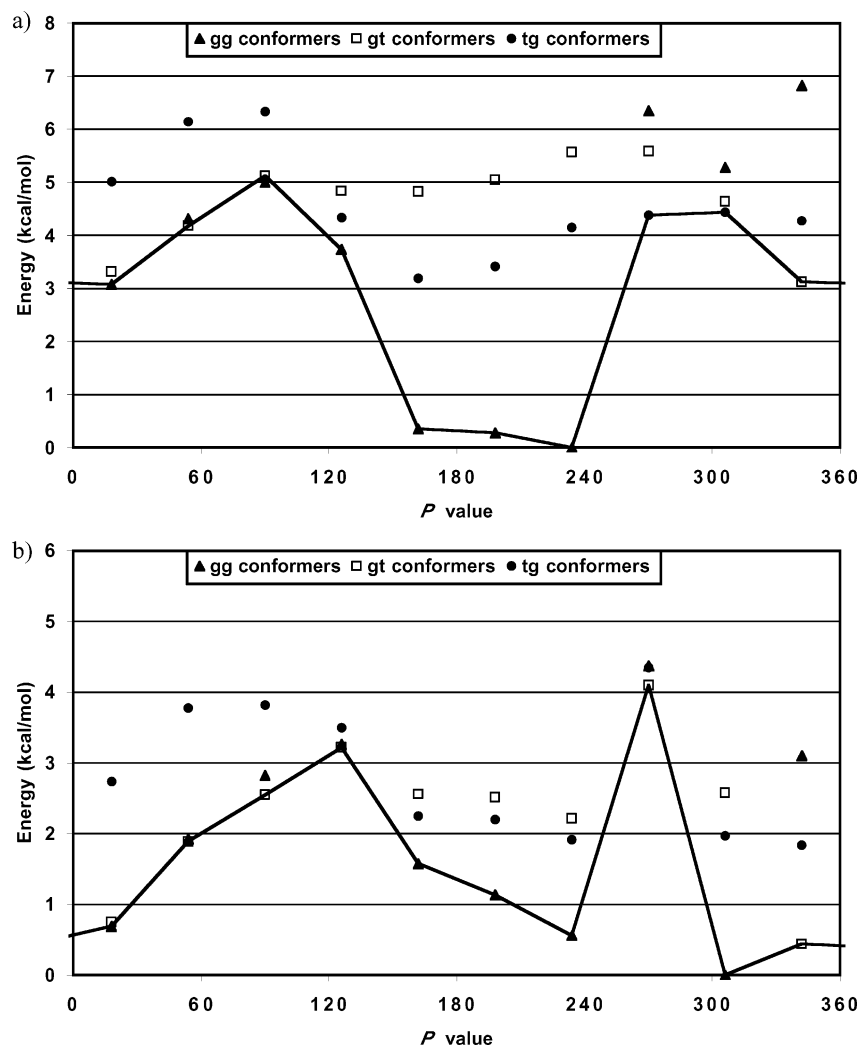


**Figure 11.** (a) Gas-phase relative energy profile of **6** at the B3LYP/6-31+G\*\*//B3LYP/6-31G\* level of theory. (b) Solution-phase relative energy profile of **6** at the B3LYP/6-31+G\*\*//SM5.42/BPW91/6-31G\* level of theory. See Figure 2 for the definitions of the gg, gt, and tg rotamers about the C<sub>4</sub>–C<sub>5</sub> bond. The line drawn connects the lowest energy rotamer for each ring form.

found the  $\Phi_m$  to be the greatest for conformers in the northeastern portion of the pseudorotational itinerary and the least for conformers in the western portion. The general energetic trends of the two studies are similar, but as the previous study was carried out on the reducing sugar, not with the methyl glycoside studied here, direct comparisons are difficult.

**G. Methyl  $\alpha$ -D-Xylofuranoside (**7**). Geometrical Preferences.** Optimization of the 30 conformers of **7** at the B3LYP/6-31G\* level of theory produced a variety of H-bonding patterns. All conformers except the <sup>2</sup>E-gg structure were stabilized by a H-bond from OH<sub>2</sub> to O<sub>1</sub>. The <sup>2</sup>E-gg conformer was also atypical in that it was the only conformer stabilized by a H-bond from OH<sub>5</sub> to O<sub>4</sub>. The only other gg and tg conformers that were not stabilized by a H-bond from OH<sub>5</sub> to O<sub>3</sub> were the <sup>3</sup>E-gg, <sup>3</sup>E-tg, and E<sub>4</sub>-gg conformers. None of the gt conformers were stabilized by a H-bond involving OH<sub>5</sub>. The <sup>2</sup>E and E<sub>3</sub> ring conformers were stabilized by an additional weak O<sub>3</sub>–H $\cdots$ O<sub>2</sub> H-bond. Optimization of the gas-phase conformers at the SM5.42/BPW91/6-31G\* level of theory produced no gross reorganization of the H-bonding patterns. The O<sub>3</sub>–H $\cdots$ O<sub>2</sub> H-bond weakened slightly as measured by an average lengthening of the distance between the hydrogen and acceptor oxygen of 0.06 Å and decrease of the H-bond angle by 2°. In contrast, the average length of the O<sub>5</sub>–H $\cdots$ O<sub>3</sub> H-bond decreased and the H-bond angle increased upon optimization, which suggests a

strengthening of this H-bond. The strength of the O<sub>2</sub>–H $\cdots$ O<sub>1</sub> H-bond appeared unchanged by optimization in the SM5.42 model of aqueous solution. Both the gas- and solution-phase structures of **7** had a small distribution of  $\Phi_m$  values (Table 1). Most conformers had a  $\Phi_m$  from 35° to 40° (see the Supporting Information), and similar to the other rings, the  $\Phi_m$  increased slightly upon optimization in the SM5.42 model of aqueous solvent (Table 1).

**Energetic Profiles.** The lowest energy structure at the B3LYP/6-31+G\*\*//B3LYP/6-31G\* level of theory was the <sup>2</sup>E-tg conformer (Figures 12a and 13a). As expected, this was one of the more highly H-bonded structures with a total of three H-bonds. Placement of both secondary hydroxyl groups in an equatorial position as well as axial arrangement of the aglycone further stabilized this conformer. The closely related E<sub>1</sub>-tg conformer was only slightly higher in energy in the gas phase. However, the structurally similar <sup>2</sup>E-gg conformer was stabilized only by a single, weak H-bond and was therefore 5.6 kcal/mol higher in energy than its counterpart with the tg orientation about the C<sub>4</sub>–C<sub>5</sub> bond. The entire northern portion of the pseudorotational itinerary was significantly higher in energy than the southern portion as a result of the equatorial placement of the aglycone and axial orientation of the secondary hydroxyl groups. The N minimum <sup>0</sup>E-tg conformer was 1.6 kcal/mol above the global minimum (Figures 12a and 13a). This conformer was stabilized by axial placement of the aglycone, equatorial

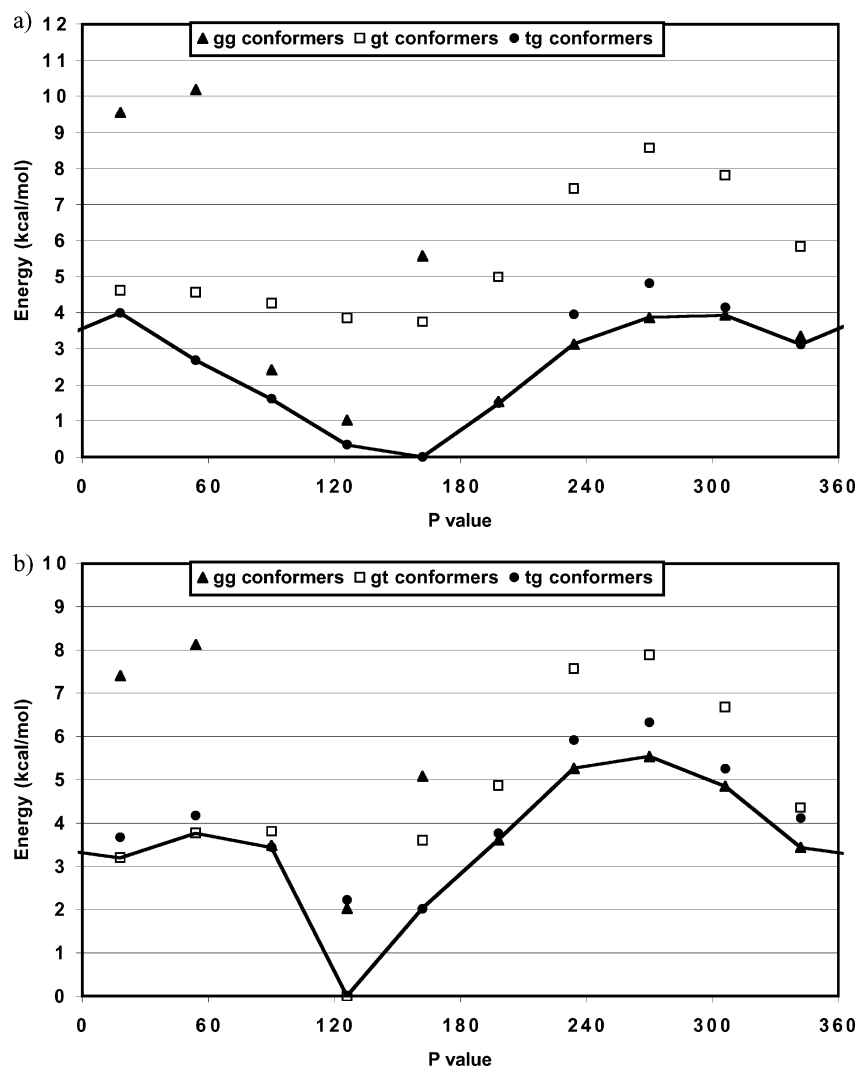


**Figure 12.** (a) Gas-phase relative energy profile of **7** at the B3LYP/6-31+G\*\*//B3LYP/6-31G\* level of theory. (b) Solution-phase relative energy profile of **7** at the B3LYP/6-31+G\*\*//SM5.42/BPW91/6-31G\* level of theory. See Figure 2 for the definitions of the gg, gt, and tg rotamers about the C<sub>4</sub>–C<sub>5</sub> bond. The line drawn connects the lowest energy rotamer for each ring form.

placement of the C<sub>4</sub>-hydroxymethyl group, and two moderate H-bonds as discussed above. The gt rotamers were substantially higher in energy than the gg and tg conformers in the gas phase because of their inability to H-bond to O<sub>3</sub>. Regardless, within the gt conformer series, the same ring conformers were found to be low-energy species.

Inclusion of solvent effects at the B3LYP/6-31+G\*\*//SM5.42/BPW91/6-31G\* level of theory caused only minor rearrangements in the energy profile compared to the gas-phase results discussed above (Figure 12). The southern ring conformers remained lowest in energy with the eastern portion of the pseudorotational itinerary slightly lower in energy than the western structures. The identity of the global minimum, however, did shift slightly to the E<sub>1</sub>-gt ring conformer (Figure 13a), as a result of the decreased importance of H-bond stabilization in the SM5.42 model for aqueous solvation. The solution-phase global minimum (E<sub>1</sub>-gt) was stabilized only by a H-bond from OH<sub>2</sub> to O<sub>1</sub>, whereas the gas-phase global minimum (<sup>2</sup>E-tg) was stabilized by three H-bonds. The gas-phase global minimum and the other two C<sub>4</sub>–C<sub>5</sub> rotamers of the solution-phase E<sub>1</sub>-gt conformer were the next lowest energy conformers in solution at approximately 2.0 kcal/mol. The axial placement of the aglycone in these two low-energy ring conformers suggests the importance of the anomeric effect in stabilization of the methyl α-D-xylofuranoside ring conforma-

tions. The N minimum was also a gt rotamer, the <sup>3</sup>E ring conformer. The E<sub>2</sub>, E<sub>4</sub>, and <sup>0</sup>E ring conformers were only, however, approximately 0.5 kcal/mol higher in energy. Among these lower energy northern structures the <sup>3</sup>E conformer was stabilized by pseudoequatorial arrangement of the C<sub>4</sub>-hydroxymethyl group and stereoelectronically preferred axial placement of the secondary hydroxyl groups. The stabilization achieved by H-bond formation appeared negligible in both northern and southern conformers as observed by the lower energy of many gt rotamers relative to gg and tg rotamers of the same ring conformation.

**Comparison to Previous Studies.** An X-ray crystal structure of **7** was recently reported showing a <sup>2</sup>E ring conformation.<sup>16</sup> The current study found this ring conformation to be the gas-phase global minimum and a low-energy structure in aqueous solution. Analysis of <sup>3</sup>J<sub>H,H</sub> data alone had been inconclusive, but analysis of <sup>3</sup>J<sub>H,H</sub> and <sup>3</sup>J<sub>C,H</sub> data indicates that **7** exists primarily as the E<sub>1</sub> ring form in aqueous solution (Table 2).<sup>4b</sup> This was also found to be a low-energy gas-phase structure and the solution-phase global minimum in the current study. Analysis of <sup>3</sup>J<sub>H,H</sub> data also suggests that less than 10% of **7** may exist as the <sup>1</sup>T<sub>2</sub> ring conformation. The current study is consistent with the proposal that the <sup>1</sup>T<sub>2</sub> ring conformation is a low-energy geometry as the envelope conformer adjacent to this twist form, E<sub>2</sub>, is the low-energy N conformer in solution.

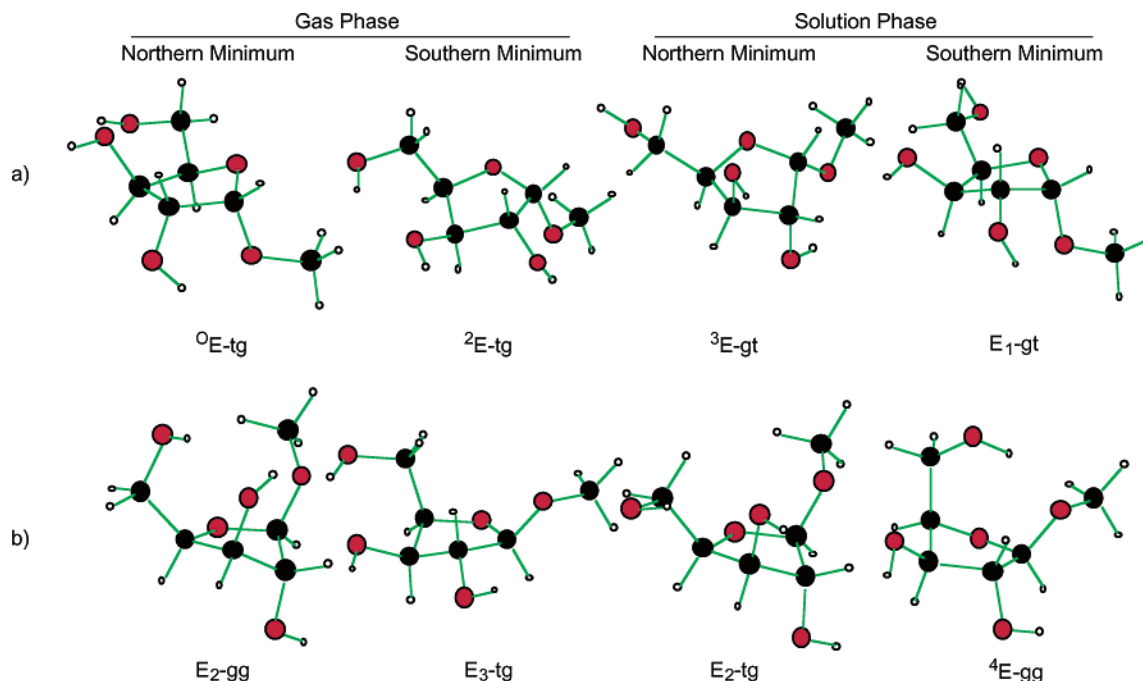


**Figure 13.** Northern and southern minima of (a) **7** and (b) **8** at the B3LYP/6-31+G\*\*//B3LYP/6-31G\* (gas) and B3LYP/6-31+G\*\*//SM5.42/BPW91/6-31G\* (solution) levels of theory.

Finally, this theoretical study confirms our earlier finding that **7** does not exist as a 2:3 mixture of the  $^1E$  and  $E_3$  ring conformations, one of two possible conformer solutions predicted by using  $^3J_{H,H}$  data alone in the conformational analyses. As shown in Figure 12, the  $^1E$  and  $E_3$  ring conformers are high-energy structures in both the gas and solution phases. To our knowledge, this is the first theoretical study of the conformational preferences of an  $\alpha$ -D-xylofuranoside.

**H. Methyl  $\beta$ -D-Xylofuranoside (**8**). Geometrical Preferences.** Optimization of the 30 envelope geometries of **8** at the B3LYP/6-31G\* level of theory produced a family of conformers with a large diversity of hydrogen-bonding patterns. The most prevalent and strongest H-bond type was between  $OH_5$  and  $O_3$ . The average length of this bond for the gg and tg rotamers was 2.05 Å, and the average bond angle was 131.1°. All of the gg and tg rotamers were stabilized by this type of H-bond except the  $^4E$ -gg and  $E_3$ -gg conformers in which  $OH_5$  was H-bonded to  $O_1$ . None of the gt rotamers were stabilized by H-bonds involving  $OH_5$ . Two conformers,  $^3E$ -gg and  $E_2$ -gg, were also stabilized by a transannular H-bond from the  $OH_3$  to  $O_1$ . The southern  $^2E$  and  $E_1$  ring conformers were further stabilized by weak  $O_2-H\cdots O_1$  and  $O_3-H\cdots O_2$  H-bonds; the  $E_3$  ring conformer was also stabilized by the latter type of H-bond. Optimization at the SM5.42/BPW91/6-31G\* level of theory produced mixed results. On average, the weak H-bonds present in the gas-phase conformers became weaker, but the moderate H-bonds became stronger. For example, the average length of the  $O_3-H\cdots O_2$  H-bond increased by 0.07 Å, while the average length of the H-bond from  $OH_5$  to  $O_3$  decreased by the same amount. The bond angles and other H-bond types indicated the same trend (see the Supporting Information). The  $\Phi_m$  of the  $\beta$ -D-xylofuranosyl ring varied from 24° to 43° (Table 1). The average  $\Phi_m$  in the gas phase was slightly less (36.4°) than for the solution-phase (36.7°) conformers of **8**.

**Energetic Profiles.** The relative energy of the conformers of **8** at the B3LYP/6-31+G\*\*//B3LYP/6-31G\* level of theory were heavily biased by H-bond strengths. The N and global minimum  $E_2$ -gg conformer was stabilized by two moderately strong

H-bonds, one from  $OH_5$  to the  $O_3$  and the other from  $OH_3$  to the  $O_1$  (Figures 13b and 14a). The other low-energy N conformer was 0.6 kcal/mol higher in energy and stabilized by the same H-bonding pattern, although the  $OH_3$  to  $O_1$  H-bond was 0.4 Å longer and 10° narrower. The S minimum was also highly stabilized by H-bonds. The  $E_3$ -tg conformer was 0.4 kcal/mol higher in energy than the global minimum, stabilized by one moderate H-bond and one weak H-bond as described above. The other low-energy southern structures were structurally similar and also stabilized by at least one moderate H-bond and one weak H-bond. Additional stabilization of the  $^2E$  and  $E_3$  ring conformers was achieved by equatorial placement of the secondary hydroxyl groups.

The solution-phase energy diagram of **8** at the B3LYP/6-31+G\*\*//SM5.42/BPW91/6-31G\* level of theory was the most featureless found in this study. The highest energy conformer was only 2.5 kcal/mol above the global minimum. Because of the similar energetics of the conformers studied, detailed analysis of the results is difficult. The energy profile suggested that the lowest energy ring conformation was in the  $^2E$  to  $^4E$  range. The other ring forms were approximately 1.0 kcal/mol higher in energy. The highest energy ring conformation was  $^0E$ , but that was only 1.4 kcal/mol above the global minimum. Therefore, analysis of Figure 14b suggested that **8** should exist in solution predominantly as a southern ring form in the  $^2E$  to  $^4E$  range. The identity of the N minimum was not clarified, although the  $^0E$  ring conformation would be the most unlikely.

**Comparison to Previous Studies.** To our knowledge, the only conformational information available to date for **8** is from analysis of  $^3J_{H,H}$  and  $^3J_{C,H}$  data in aqueous solution.<sup>4b</sup> Analysis of these data found the N minimum to be the  $E_2$  ring conformer and the S minimum to be either the  $^4T_O$  or  $E_O$  ring conformer depending upon the number of data points used in the analysis. The theoretical approach reported here found an  $E_2$  ring conformer to be the global minimum in the gas phase and the N minimum in solution. Both the gas- and solution-phase results found the  $^4E$  ring conformers to be lower in energy than the  $E_O$  ring conformers, suggesting that **8** most likely exists as a 4:1



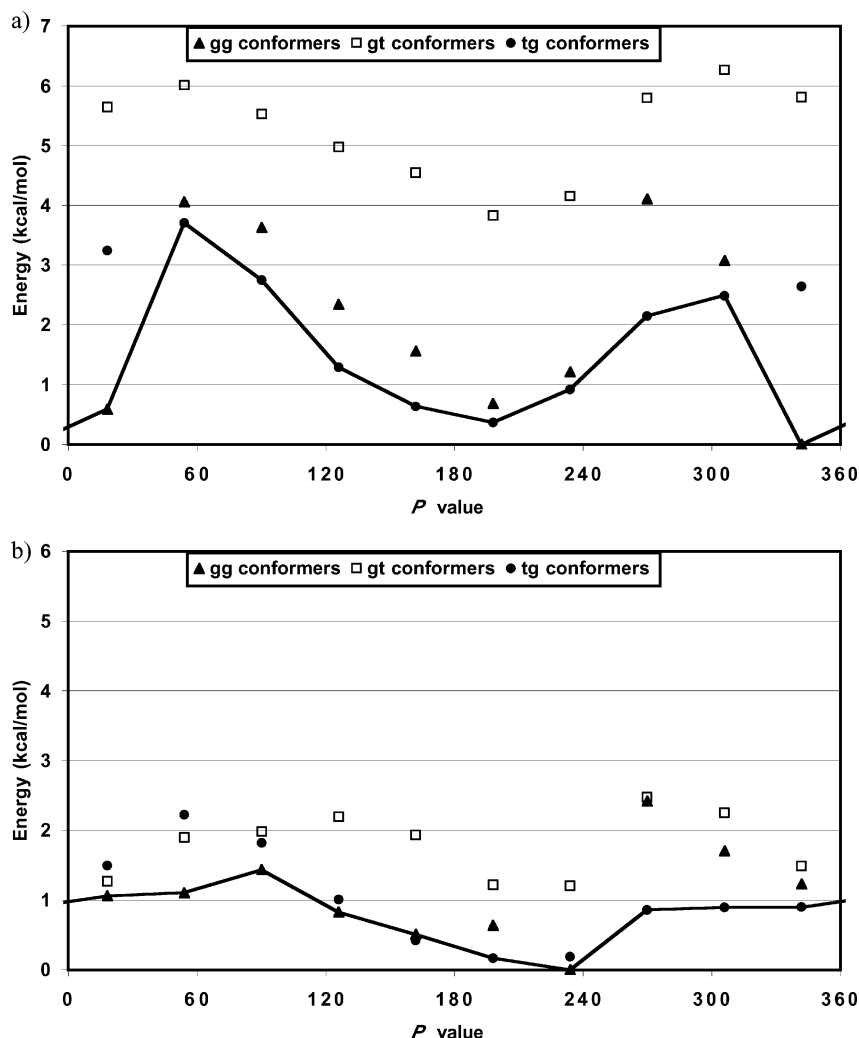


**Figure 14.** (a) Gas-phase relative energy profile of **8** at the B3LYP/6-31+G\*\*//B3LYP/6-31G\* level of theory. (b) Solution-phase relative energy profile of **8** at the B3LYP/6-31+G\*\*//SM5.42/BPW91/6-31G\* level of theory. See Figure 2 for the definitions of the gg, gt, and tg rotamers about the C<sub>4</sub>–C<sub>5</sub> bond. The line drawn connects the lowest energy rotamer for each ring form.

ratio of the E<sub>2</sub> and <sup>4</sup>T<sub>O</sub> ring conformations as suggested by analysis of all available variable-temperature <sup>3</sup>J<sub>H,H</sub> data (Table 2).<sup>4b</sup>

## Conclusions

In this paper we have detailed the conformational preferences of the furanose ring in **1–8** in both the gas (B3LYP/6-31+G\*\*//B3LYP/6-31G\*) and aqueous solution (B3LYP/6-31+G\*\*//SM5.42/BPW91/6-31G\*) phases. Detailed analysis of the geometrical and energetic data revealed the following.

(1) Intramolecular H-bonds of moderate strength in the gas phase remained geometrically important in the SM5.42 model of aqueous solution, although the energetic stability derived from these H-bonds was significantly reduced in solution. H-bonds that were weak in the gas phase generally weakened further upon optimization in solution as measured by the length and angle of the H-bonds. Interestingly, however, stronger hydrogen bonds in the gas phase (shorter and more linear) generally became stronger upon SM5.42 optimization.

(2) The  $\Phi_m$  of most furanose rings did vary as a function of  $P$  value with ring conformers from  $P = 18^\circ$  to  $P = 90^\circ$  having the largest  $\Phi_m$  and ring conformers from  $P = 161^\circ$  to  $P = 270^\circ$  having the smallest. The ring systems in which this was most pronounced were **1**, **5**, and **6**.

(3) When the gas-phase and solution  $\Phi_m$  values are compared, the latter are slightly larger. This is consistent with decreased intramolecular hydrogen bonding, which provides greater flexibility to the ring.

(4) The  $\Phi_m$  values of the furanose ring in low-energy gas- and solution-phase conformers of **1–8** correspond well with those seen in available crystal structures.

(5) Substantial agreement exists between the results of this theoretical study and those from previous experimental studies. We propose, therefore, the solution-phase conformational preferences of all eight natural aldopentofuranosides can now be assigned with reasonable confidence (Table 2).

These findings will enable further experimental studies of furanose ring conformation in more complicated and larger carbohydrate systems. Furthermore, the important structural role played by H-bonds, even in solution, requires further analysis.

**Acknowledgment.** This work was funded by grants from the National Science Foundation (CHE-9875163 and CHE-9733457) and the Ohio Supercomputer Center. J.B.H. was supported as a graduate research fellow by an NIH Training Grant for Chemistry at the Biology Interface. We thank Professors Christopher Cramer and Donald Truhlar (Minnesota) for access to the MN-GSM solvation code.

**Supporting Information Available:** Tables of H-bonds present in **1–8** and tables and graphs demonstrating the dependence of  $\Phi_m$  upon  $P$  value and energy. This material is available free of charge via the Internet at <http://www.acs.org>.

## References and Notes

- (1) (a) Esposito, L.; Vitagliano, L.; Mazzarella, L. *Protein Pept. Lett.* **2002**, *9*, 95. (b) Smyth, M. S.; Martin, J. H. J. *Mol. Path.* **2000**, *53*, 8. (c) Mollova, E. T.; Pardi, A. *Curr. Opin. Struct. Biol.* **2000**, *10*, 298. (d) Matthews, S. J. *Nucl. Magn. Reson.* **2002**, *31*, 312. (e) Foloppe, N.; Nilsson, L.; MacKerell, A. D., Jr. *Biopolymers* **2001**, *61*, 61. (f) Hardin, C.; Pogorelov, T. V.; Luthey-Schulten, Z. *Curr. Opin. Struct. Biol.* **2002**, *12*, 176.
- (2) Galan, M. C.; Venot, A. P.; Glushka, J.; Imberty, A.; Boons, G.-J. *J. Am. Chem. Soc.* **2002**, *124*, 5964.
- (3) (a) Ford, H., Jr.; Dai, F.; Mu, L.; Siddiqui, M. A.; Nicklaus, M. C.; Anderson, L. Marquez, V. E.; Barchi, J. J., Jr. *Biochemistry* **2000**, *39*, 2581. (b) Marquez, V. E.; Wang, P.; Nicklaus, M. C.; Maier, M.; Manoharan, M.; Christman, J. K.; Banavali, N. K.; Mackerell, A. D., Jr. *Nucleosides, Nucleotides, Nucleic Acids* **2001**, *20*, 451. (c) Jacobson, K. A.; Ravi, R. G.; Nandan, E.; Kim, H. S.; Moro, S.; Kim, Y. C.; Lee, K.; Barak, D.; Marquez, V. E.; Ji, X. D. *Nucleosides, Nucleotides, Nucleic Acids* **2001**, *20*, 333. (d) Meier, C.; Knispel, T.; Marquez, V. E.; De Clercq, E.; Balzarini, J. *Nucleosides Nucleotides* **1999**, *18*, 907.
- (4) (a) Houseknecht, J. B.; Altona, C.; Hadad, C. M.; Lowary, T. L. *J. Org. Chem.* **2002**, *67*, 4647. (b) Houseknecht, J. B.; Hadad, C. M.; Lowary, T. L. *J. Phys. Chem. A* **2003**, *107*, 372. (c) Gordon, M. T.; Lowary, T. L.; Hadad, C. M. *J. Am. Chem. Soc.* **1999**, *121*, 9682. (d) Gordon, M. T.; Lowary, T. L.; Hadad, C. M. *J. Org. Chem.* **2000**, *65*, 4954. (e) McCarren, P. R.; Gordon, M. T.; Lowary, T. L.; Hadad, C. M. *J. Phys. Chem. A* **2001**, *105*, 5911. (f) Houseknecht, J. B.; McCarren, P. R.; Lowary, T. L.; Hadad, C. M. *J. Am. Chem. Soc.* **2001**, *123*, 8811. (g) Callam, C. S.; Singer, S. J.; Lowary, T. L.; Hadad, C. M. *J. Am. Chem. Soc.* **2001**, *123*, 11743. (h) D'Souza, F. W.; Ayers, J. D.; McCarren, P. R.; Lowary, T. L. *J. Am. Chem. Soc.* **2000**, *122*, 1251. (i) Houseknecht, J. B.; Lowary, T. L. *J. Org. Chem.* **2002**, *67*, 4150.
- (5) Brennan, P. J.; Nikaido, H. *Annu. Rev. Biochem.* **1995**, *64*, 29.
- (6) (a) Kilpatrick, J. E.; Pitzer, K. S.; Spitzer, R. *J. Am. Chem. Soc.* **1947**, *69*, 2483. (b) Pitzer, K. S.; Donath, W. F. *J. Am. Chem. Soc.* **1959**, *81*, 3213. (c) Altona, C.; Sundaralingam, M. *J. Am. Chem. Soc.* **1972**, *94*, 8205. (d) Altona, C.; Sundaralingam, M. *J. Am. Chem. Soc.* **1973**, *95*, 2333.
- (7) (a) Serianni, A. S.; Chipman, D. M. *J. Am. Chem. Soc.* **1987**, *109*, 5297. (b) Church, T. J.; Carmichael, I.; Serianni, A. S. *J. Am. Chem. Soc.* **1997**, *119*, 8946.
- (8) (a) PSEUROT 6.2, 1993; PSEUROT 6.3, 1999: van Wijk, J.; Haasnoot, C. A. G.; de Leeuw, F. A. A. M.; Huckriede, B. D.; Westra Hoekzema, A.; Altona, C., Leiden Institute of Chemistry, Leiden University, Leiden, The Netherlands. (b) de Leeuw, F. A. A. M.; Altona, C. *J. Comput. Chem.* **1983**, *4*, 428. (c) Altona, C. *Recl. Trav. Chem. Pays-Bas* **1982**, *101*, 413.
- (9) Frisch, M. J.; Trucks, G. W.; Schlegel, H. B.; Scuseria, G. E.; Robb, M. A.; Cheeseman, J. R.; Zakrzewski, V. G.; Montgomery, J. A., Jr.; Stratmann, R. E.; Burant, J. C.; Dapprich, S.; Millam, J. M.; Daniels, A. D.; Kudin, K. N.; Strain, M. C.; Farkas, O.; Tomasi, J.; Barone, V.; Cossi, M.; Cammi, R.; Mennucci, B.; Pomelli, C.; Adamo, C.; Clifford, S.; Ochterski, J.; Petersson, G. A.; Ayala, P. Y.; Cui, Q.; Morokuma, K.; Malick, D. K.; Rabuck, A. D.; Raghavachari, K.; Foresman, J. B.; Cioslowski, J.; Ortiz, J. V.; Stefanov, B. B.; Liu, G.; Liashenko, A.; Piskorz, P.; Komaromi, I.; Gomperts, R.; Martin, R. L.; Fox, D. J.; Keith, T.; Al-Laham, M. A.; Peng, C. Y.; Nanayakkara, A.; Gonzalez, C.; Challacombe, M.; Gill, P. M. W.; Johnson, B.; Chen, W.; Wong, M. W.; Andres, J. L.; Gonzalez, C.; Head-Gordon, M.; Replogle, E. S.; Pople, J. A. *Gaussian 98*, Revision A.9; Gaussian, Inc.: Pittsburgh, PA, 1998.
- (10) Cramer, C. J.; Truhlar, D. G. *Chem. Rev.* **1999**, *99*, 2161.
- (11) (a) Becke, A. D. *Phys. Rev. A* **1988**, *38*, 3098. (b) Becke, A. D. *J. Chem. Phys.* **1993**, *98*, 5648. (c) Lee, C.; Yang, W.; Parr, R. G. *Phys. Rev. B* **1988**, *37*, 785.
- (12) (a) Kidos, J. D.; Li, J.; Hawkins, G. D.; Liotard, D. A.; Cramer, C. J.; Truhlar, D. G.; Frisch, M. J. *MN-GSM*, version 99.2; University of Minnesota: Minneapolis, MN. (b) Li, J.; Zhu, T.; Cramer, C. J.; Truhlar, D. G. *J. Phys. Chem. A* **1998**, *102*, 1820. (c) Li, J.; Hawkins, G. D.; Cramer, C. J.; Truhlar, D. G. *Chem. Phys. Lett.* **1998**, *288*, 293. (d) Zhu, T.; Li, J.; Hawkins, G. D.; Cramer, C. J.; Truhlar, D. G. *J. Chem. Phys.* **1998**, *109*, 9117. (e) Li, J.; Zhu, T.; Hawkins, G. D.; Winget, P.; Liotard, D. A.; Cramer, C. J.; Truhlar, D. G. *Theor. Chem. Acc.* **1999**, *103*, 9.
- (13) Lemieux, R. U.; Koto, S. *Tetrahedron* **1974**, *30*, 1933.
- (14) (a) Lii, J. H.; Ma, B.; Allinger, N. L. *J. Comput. Chem.* **1999**, *15*, 1593. (b) Csonka, G.; Éliás, K.; Csizmadia, I. G. *J. Comput. Chem.* **1996**, *18*, 330. (c) Csonka, G. I.; Éliás, K.; Kolossváry, I.; Sosa, C. P.; Csizmadia, I. G. *J. Phys. Chem. A* **1998**, *102*, 1219. (d) Csonka, G. I.; Kolossváry, I.; Császár, P.; Éliás, K.; Csizmadia, I. G. *J. Phys. Chem. A* **1998**, *102*, 1219. (e) Del Bene, J. E.; Person, W. B.; Szczepaniak, K. J. *Phys. Chem.* **1995**, *99*, 10705.
- (15) ConforMole: McCarren, P. R., The Ohio State University, Columbus, OH. This program is available upon request.
- (16) Evdokimov, A.; Gilboa, A. J.; Koetzle, T. F.; Klooster, W. T.; Schultz, A. J.; Mason, S. A.; Albinati, A.; Frolow, F. *Acta Crystallogr., B* **2001**, *57*, 213.
- (17) Cros, S.; Hervé du Penhoat, C.; Pérez, S.; Imberty, A. *Carbohydr. Res.* **1993**, *218*, 81.
- (18) Evdokimov, A. G.; Martin, J. M. L.; Kalb, A. J. *J. Phys. Chem. A* **2000**, *104*, 5291.